DOI: 10.2478/ata-2019-0007

Acta Technologica Agriculturae 2
Nitra, Slovaca Universitas Agriculturae Nitriae, 2019, pp. 38–42

AN ASSESSMENT OF ANAEROBIC THERMOPHILIC CO-DIGESTION OF DAIRY CATTLE MANURE AND SEPARATED TOMATO GREENHOUSE WASTE IN LAB-SCALE REACTORS

Đurđica KOVAČIĆ*, Davor KRALIK, Daria JOVIČIĆ, Robert SPAJIĆ

J. J. Strossmayer University of Osijek, Osijek, Croatia

Anaerobic co-digestion of dairy cow manure (DCM) and separated tomato greenhouse waste (tomato stalks and leaves (TSL) and rotten and damaged tomato fruits – TF) was conducted under batch thermophilic conditions (T = 55 °C) for period of 45 days. Concentrations of substrates (tomato waste) were 5 and 10% (w/v). Each substrate, as well as experimental mixtures, was analysed in order to specify the content of pH, total solids (TS), volatile solids (VS), total extractable nitrogen (TN) and total organic carbon (TOC). Biogas yield and composition, as well as cumulative biogas curves, were reported. In comparison to DCM monodigestion (329.5 $cm^3 \cdot g^{-1}$ VS), biogas yield was significantly improved in experiment C (365.1 $cm^3 \cdot g^{-1}$ VS) (with 5% (w/v) TF added), whereas methane yield did not show any significant difference. Experiment D (with 10% (w/v) TSL added) resulted in significantly lower biogas and methane yields in contrast to the rest of experiments performed. Average methane content in all analysed experimental samples ranged from 65 to 69%. It is evident from the results that biogas production can be improved by addition of separated tomato greenhouse waste to DCM process and issue of organic waste disposal could be effectively solved.

Keywords: anaerobic co-digestion; biogas; dairy cow manure; methane; tomato greenhouse waste

In recent years, increasing attention has been paid to the proper care and management of organic agricultural waste and residuals. Scientists from all over the world are striving to develop technologies of waste management that would be simple to introduce to everyday life and would also be economical for use, as well as would be safe for both human health and environment. Biogas production utilizing waste treatment and recycling or composting can reduce pollution and disease transfer (Chongrak, 2007). Biogas production by means of anaerobic digestion provides essential benefits in contrast to other forms of bioenergy production, since it is considered a complete waste-to-energy transformation (Adekunle and Okolie, 2015; Cavinato et al., 2010). Due to its beneficial properties, various types of manure are commonly utilized as the base substrate in anaerobic digestion process (Nghiem et al., 2017, Kažímírová et al., 2018). However, digesting manure alone may not represent the most efficient way to produce biogas. One of the approaches for improving the manure digestion is to increase the biogas production rate by co-digesting it with other kinds of waste to achieve synergistic effects: balancing the C/N ratio, macro and micronutrients, pH, inhibitors/toxic compounds and total solids (TS) or volatile solids (VS) content (Li et al., 2011; Wang et al., 2014; Kovačić et al., 2017). There have been conducted numerous studies dealing with co-digestion of various organic wastes with dairy cow manure (DCM), e.g. food wastes (Li et al., 2010; Luo and Angelidaki, 2013; Zarkadas et al., 2015), harvest residues (Wang et al., 2012; Yue et al., 2013; Li et al., 2014; Kovačić et al., 2018), wastewaters and effluents (Ogejo and Li, 2010; O-Thong et al., 2012; Siddiq et al., 2014). However, there is scarcity of information on anaerobic co-digestion of separated tomato greenhouse waste with different types of manure and its potential for utilization in biogas production. Li et al. (2016) conducted solid-state anaerobic co-digestion of tomato residues with dairy manure and corn stover (11 different substrate ratios) under mesophilic regime during 45 days. Results showed improved methane yield (415.4 $cm^3 \cdot g^{-1}$ VS_{feed}) after co-digestion at ratio of 33% corn stover, 54% dairy manure and 13% tomato residues (wet base), with a reference to 0.5–10.2-fold higher yields than that of individual feedstock. Production inhibition of volatile fatty acids took place at content of tomato residues exceeding 40%. Mishra and Tenneti (2015) anaerobically co-digested tomato waste and cow dung as substrate and inoculum, respectively, in batch mesophilic and semi-continuous reactors at various hydraulic retention times. Maximum specific biogas production of 170 $cm^3 \cdot g^{-1}$ VS per day was observed during the second week of continuous operation. Saev et al. (2009) performed anaerobic co-digestion of tomato waste and cattle manure in semi-continuous mode at mesophilic conditions. The average biogas yield was 220 $cm^3 \cdot g^{-1}$ VS, while maximal methane production in total was achieved when the ratio of cattle manure/tomato waste was 80 : 20 and organic loading rate was 2.9 kg VS $m^{-3} \cdot d^{-1}$. Saghouri et al. (2018) conducted anaerobic co-digestion of waste from tomato processing in lab-scale batch mesophilic reactors with continuous mixing lasting 48 days. Slurry of digested

Contact address: Đurđica Kovačić, J. J. Strossmayer University of Osijek, Faculty of Agrobiotechnical Sciences Osijek, Vladimira Preloga 1, HR - 31000 Osijek, Croatia, e-mail: durda7@gmail.com

cattle manure was used as inoculum. The highest produced biogas yield was 140 $cm^3 \cdot g^{-1}$ VS and highest methane content was 60.5% in produced biogas.

Addition of vegetable waste to DCM can be a suitable option for improving the process of anaerobic digestion. Manure usually provides good buffering capacity and contains all nutrients required by the anaerobic bacteria, especially nitrogen (Nghiem et al., 2017; Wang et al., 2014; Zhang et al., 2017). Vegetable waste has high moisture content (75–90%) and is highly biodegradable, which encourages the rapid production of volatile fatty acids. These acids lead to a rapid pH drop, which may inhibit methanogenic activity. Moreover, vegetable waste is low in nitrogen and phosphorus, which may result in low methane yield when monodigested. Therefore, mixing it with other wastes, such as manure, which has higher nitrogen content, is preferable. In such manner, system acidification can be avoided (Tarekegn and Abebe, 2017; Siripong and Dulyakasem, 2012).

Aim of this work was to investigate the anaerobic co-digestion potential of separated tomato greenhouse waste residues with DCM under batch thermophilic regime, in which tomato greenhouse waste was added to DCM in two different proportions.

Material and methods

Substrates

Industrial waste in the production of tomatoes (stalks, leaves, rotten and damaged tomato fruits) used in this study was collected from the greenhouse "Magadenovac" (Slavonia and Baranja County, Croatia); it was stored in a freezer at -20 °C for later use. Tomato samples were defrosted at 4 °C for 24 h, oven dried at 60 °C for 24 h, pruned into pieces with length of 3–5 cm and finally ground and homogenized in a kitchen blender. DCM was obtained from local dairy farm Topolik (Slavonia and Baranja County, Croatia). Fresh manure was obtained in 15 dm^3 plastic pails. These were delivered to the laboratory just before the commencement of experiment for the purposes of inoculum.

Analytical methods

Each substrate and inoculum were analysed for pH, TS, VS, TOC and TN, which were measured in accordance with the standard methods (APHA, 1998). The pH was measured using a portable pH meter and combination glass electrode (Mettler Toledo Five Easy, Switzerland) at room temperature. The pH of ground tomato substrates was specified from suspension obtained by weighing 1 g of substrate. Subsequently, 20 cm^3 of distilled water was added to it. Final pH results were shown after 30 min. TS content was determined when weight showed no further changes during drying process at 105 °C in the laboratory oven (Memmert UFE 600, Germany). Considering the VS content, it was determined by means of complete combustion in a muffle furnace that lasted for 4 h at 550 °C. Kjeldahl method (Büchi digestion unit K-437, Büchi distillation unit B-324, Switzerland) was utilized for determination of TN content. TOC content was specified in accordance with an international standardization operation method (ISO 14235, 1998) (UV-VIS spectrophotometer Cary 50, Varian, Australia).

Sampling and biogas composition analyses were conducted on daily basis until the methanogenesis commencement. Subsequently, sampling and biogas composition analyses were performed on every fourth day. A modified method (HRN ISO 6974-4:2000) using a GC (Varian 3900, USA) equipped with capillary column CP-PoraPLOT Q fused silica PLOT 25 × 0.53 mm, df = 20 µm was utilized in order to analyse the biogas composition.

Lab-scale batch anaerobic co-digestion

Ground tomato substrates were homogenized with DCM prior to anaerobic batch co-digestion. Experiments were carried out under thermophilic conditions (T = 55 °C) for period of t = 45 days in apparatus described in our previous research (Kovačić et al., 2018).

Reaction mixture was of total volume of 500 cm^3. The substrates concentrations were 5 and 10% (w/v). Each experiment was triplicated. Content of each reactor was subtly mixed manually five times a day in order to ensure homogeneity. Furthermore, single DCM was digested as well in order to provide control and comparison sample. The experimental design is shown in Table 1.

Table 1 Experimental design

Experiment	Composition of experimental sample	Mixture symbol
Inoculum	DCM	A
1	DCM + TSL 5% (w/v)	B
2	DCM + TF 5% (w/v)	C
3	DCM + TSL 10% (w/v)	D
4	DCM + TF 10% (w/v)	E

DCM – dairy cow manure, TF – tomato fruits, TSL – tomato stalks and leaves

Statistical analysis

Statistical analysis of biogas and methane yields was done according to analysis of variance (ANOVA) by means of SAS software for Windows (SAS Institute Inc., Cary, NC, USA). In case of occurrence of statistically significant differences (p <0.05), the means were subsequently separated by means of Fisher's multiple range test. All results provided are mean values.

Results and discussion

In this research, addition of separated tomato greenhouse waste (TSL and rotten and damaged TF) to DCM was evaluated in order to conduct the process of anaerobic co-digestion. As far as it is possible to claim, this is the first attempt to perform batch anaerobic co-digestion of separated tomato greenhouse waste and DCM under thermophilic regime.

Main substrate properties are shown in Table 2.

Addition of acidic tomato greenhouse waste slightly lowered pH value of experimental mixtures (pH

Table 2 Main properties of raw substrates and inoculum

	pH	TS (%)*	VS (%)**	Ash (%)**	TN (%)**	TOC (%)**	C/N
Raw substrates and inoculum							
DCM	7.03 ±0.01	6.58 ±0.07	84.51 ±0.55	15.49	4.56 ±0.02	37.78 ±0.27	8.3
TSL	5.12 ±0.03	12.52 ±0.25	86.60 ±0.20	13.40	2.27 ±0.04	41.47 ±0.34	18.3
TF	4.03 ±0.03	7.63 ±0.23	93.21 ±0.14	6.79	3.46 ±0.03	44.30 ±0.25	12.8
Experimental mixtures							
B	6.75 ±0.00	7.00 ±0.07	84.02 ±0.66	15.31	3.84 ±0.34	38.24 ±0.80	10.0
C	6.70 ±0.01	6.56 ±0.04	83.63 ±0.40	13.87	3.92 ±0.21	41.67 ±0.23	10.6
D	6.61 ±0.07	8.50 ±1.12	86.58 ±0.24	13.46	3.57 ±0.03	39.14 ±0.66	11.0
E	6.53 ±0.04	6.80 ±0.04	86.78 ±0.18	12.22	3.74 ±0.17	42.06 ±0.54	11.2

* – based on wet weight; ** – based on dry weight

6.5–7.7) making the mixtures still sufficiently amenable to methanogenic bacteria and thus allowing them to function properly and attain maximal biogas yield (Tarekegn and Abebe, 2017; Khalid et al., 2011). C/N ratio is another important factor that affects process of biogas production. Siddiqui et al. (2011) reported ideal C/N ratio within the range of 9 to 30. C/N ratio in DCM was quite low (approx. 8). On the contrary, it was higher (approx. 18 and 12, respectively) in tomato green parts and fruits. Thereby, by addition of tomato residues to manure, there was an increase in C/N ratio in all prepared experimental mixtures (to approx. 10–11), resulting in more favourable media for methanogens.

Daily biogas production curves are presented in Fig. 1. General variation is evident between samples containing 5 and 10% (w/v) tomato residues. Methanogenesis progress was quite similar in experiments containing 5% (w/v) tomato residues and experiment containing pure manure. Several peak values were recorded for all three experiments during observed period (experiments A, B and C).

The highest biogas production in reactor containing DCM started on the 8th day of the process and lasted for 8 days. However, in experiments containing tomato residues, beginning of highest biogas production varied between the samples. The highest biogas production started on the 11th and 7th day of the process and dynamic phase of biogas production lasted for 8 and 7 days in experiment B and C, respectively.

However, addition of 10% (w/v) tomato residues to manure resulted in more equable process without multiple peak values and beginning of higher biogas production started quite later on – on the 23rd and 13th day in experiments D and E, respectively. That dynamic phase of biogas production lasted for 4 and 6 days, respectively, implying that biogas production was more balanced throughout the process in contrast to experiments containing 5% (w/v) tomato residues added.

After anaerobic co-digestion of DCM and tomato greenhouse waste residuals, average cumulative biogas yields (Fig. 2) were specified.

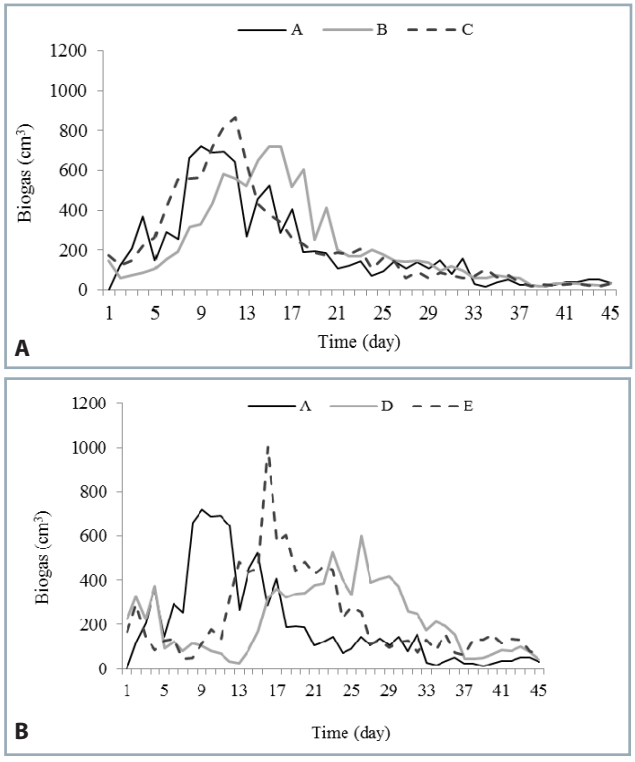

Fig. 1 Daily biogas production during anaerobic co-digestion of DCM and tomato greenhouse waste residuals added: A) 5% (w/v) added; B) 10% (w/v) added

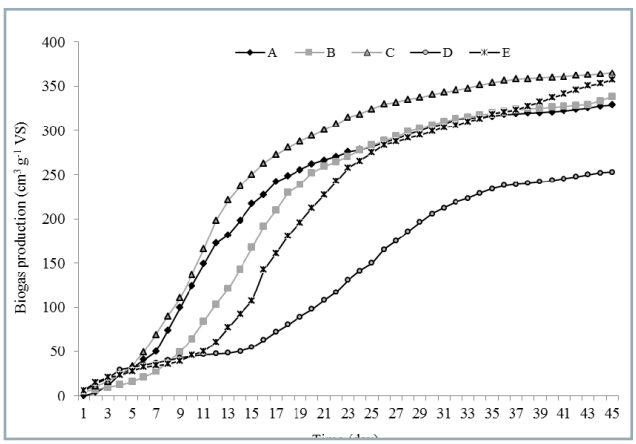

Fig. 2 Average cumulative biogas yields after anaerobic co-digestion of DCM and greenhouse waste residuals

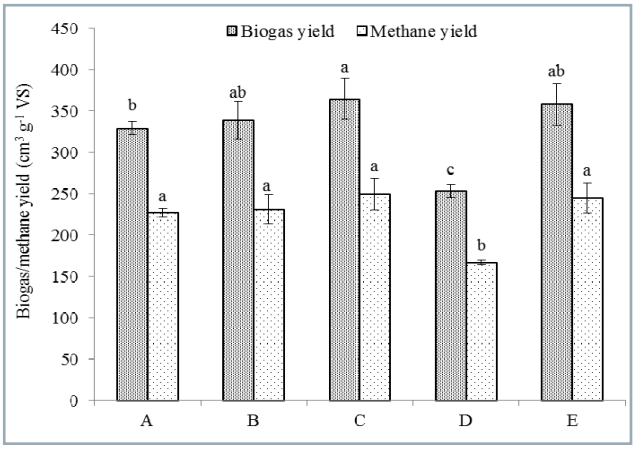

Fig. 3 Biogas and methane yields obtained from co-digested experimental samples; standard deviation is indicated by error bars ($n = 3$)

Average cumulative biogas yields obtained in experiments B, C and E were higher in contrast to DCM monodigestion by 2.7, 9.8 and 7.8%, respectively, whereas in experiment C, the highest biogas production was specified during entire process. Moreover, in terms of biogas yield, statistically significant difference was shown solely in experiment C in comparison to all other experiments (Fig. 3).

Furthermore, comparing it to the rest of experiments conducted, experiment D showed quite lower biogas production, which can be probably associated to overly high concentration of hardly/slowly degradable carbohydrates and fibres in TSL. Moreover, experiment D showed significantly lower biogas yield as well as and methane yield in contrast to all other experiments (Fig. 3).

Biogas and methane yields obtained from each experimental mixture are provided in Fig. 4. Biogas and methane yields achieved after anaerobic DCM monodigestion (experiment A) were 329.5 and 227.2 $cm^3 \cdot g^{-1}$ VS, respectively. Statistically significant ($p > 0.05$) improvement in biogas yield was gained in experiment C (365.1 $cm^3 \cdot g^{-1}$ VS) in contrast to experiment A. However, methane yield, which was 249.7 $cm^3 \cdot g^{-1}$ VS (9.0% higher in comparison to monodigested DCM), resulted in no significant difference. There was not observed any statistically significant difference in biogas yield increase between all other experiments and experiment A. However, all experiments showed more efficient biogas and methane yields in contrast to monodigested DCM. Experiments B and E resulted in 2.8 and 2.7%, and 8.1 and 4.2% higher biogas and methane yields, respectively. Experiment D showed statistically significant lower biogas and methane yields (253.5 and 166.7 $cm^3 \cdot g^{-1}$ VS, respectively) in contrast to the rest of other experiments conducted.

If compared to monodigested DCM, higher methane production was recorded in experimental samples containing tomato greenhouse waste residuals (B, C, D, E) during almost the entire process. Methane content observed in produced biogas ranged from 65 to 69% in all experimental samples.

There is not much research in literature available regarding co-digestion of tomato greenhouse waste and DCM. Saghouri et al. (2018) anaerobically digested waste from tomato processing

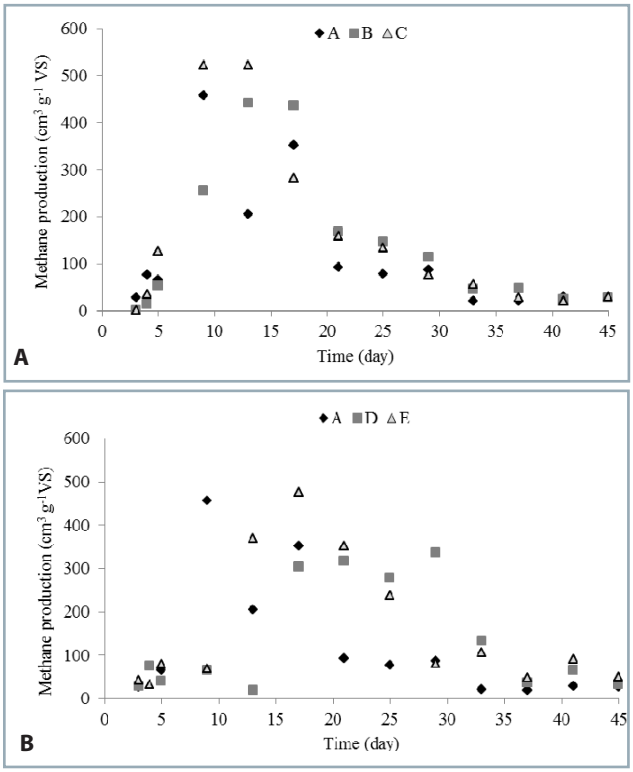

Fig. 4 Biogas and methane content produced by means of anaerobic co-digestion of dairy manure and tomato greenhouse waste residuals: A) 5% (w/v) added, B) 10% (w/v) added

using the slurry of digested cow dung as inoculum. The research was conducted in single-stage batch digester with continuous mixing under mesophilic conditions for 45 days and resulting in 140 $cm^3 \cdot g^{-1}$ VS (with 60% methane content), which is quite low in comparison to biogas yields obtained in this research after anaerobic co-digestion experiments. Furthermore, Sarada and Joseph (1996) conducted a study in order to compare single and two stage processes for methane production from waste from tomato processing under mesophilic conditions. Authors examined the factors having impact on the total biogas yield, such as loading rate, hydraulic retention time and temperature during the digestion process. The highest biogas yield reported (800 $cm^3 \cdot g^{-1}$ VS, 65% methane content) was gained on the 24th day of hydraulic retention time, at 4.5 $kg \cdot m^{-3}$ loading rate and temperature of 35 °C, resulting in 40–50% increment in both rate and yield of methane, as well as total biogas production in contrast to the single stage process under similar regime. Saev et al. (2009) examined anaerobic co-digestion of different mixtures of waste from tomato processing and cattle manure in semi-continuous lab-scale reactor under mesophilic regime and at hydraulic retention time of 20 days. The highest biogas yield (400 $cm^3 \cdot g^{-1}$ VS) and methane yield (220 $cm^3 \cdot g^{-1}$ VS) was achieved after co-digestion of mixing ratio 80 : 20 (cattle manure : diluted tomato waste) and 20:80 (cattle manure : tomato waste), respectively.

Conclusion

Addition of separated tomato greenhouse waste (TSL and rotten and damaged TF) to DCM was studied in order to assess the effect of anaerobic co-digestion efficiency. Two

different proportions (5% and 10% (w/v)) of tomato waste residues were added to DCM with aim to enhance biogas production process.

Anaerobic co-digestion of tomato greenhouse waste and DCM (experiments B, C and E) resulted in more efficient process in comparison to DCM monodigestion. Experiment C resulted in significantly improved biogas yield (9.8%) in comparison to DCM monodigestion. However, methane yield was not statistically significantly improved – there was observed 9.0% increment in methane yield.

Experiment B and E resulted in 2.8 and 2.7%, and 8.1 and 4.2% higher biogas and methane yields, respectively.

It was solely the experiment D that showed lower results in both biogas and methane yields (23.1 and 26.6%, respectively) in contrast to DCM monodigestion.

References

ADEKUNLE, K. F. – OKOLIE, J. A. 2015. A review of biochemical process of anaerobic digestion. In Advances in Bioscience and Biotechnology, vol. 6, pp. 205–212.

AMERICAN PUBLIC HEALTH ASSOCIATION (APHA). 1998. Standard Methods for the Examination of Water and Wastewater. 20th ed., Washington DC, USA.

CAVINATO, C. – FATONE, F. – BOLZONELLA, D. – PAVAN, P. 2010. Thermophilic anaerobic co-digestion of cattle manure with agro-wastes and energy crops: Comparison of pilot and full scale experiences. In Bioresource Technology, vol. 101, pp. 545–550.

CHONGRAK, P. 2007. Organic Waste Recycling: Technology and Management. London : IWA Publishing.

ISO 14235. 1998. Soil quality – Determination of organic carbon by sulfochromic oxidation.

KAŽÍMÍROVÁ, V. – GADUŠ, J. – GIERTL, T. 2018. Verification of suitability of substrate composition for production and quality of biogas. In Acta Technologica Agriculturae, vol. 21, no. 3, pp. 115–118.

KHALID, A. – ARSHAD, M. – ANJUM, M. – MAHMOOD, T. – DAWSON, L. 2011. The anaerobic digestion of solid organic waste. In Waste Management, vol. 31, no. 8, pp. 1737–1744.

KOVAČIĆ, Đ. – KRALIK, D. – JOVIČIĆ, D. – RUPČIĆ, S. – POPOVIĆ, B. – TIŠMA, M. 2018. Thermal pretreatment of harvest residues and their use in anaerobic co-digestion with dairy cow manure. In Applied Biochemistry and Biotechnology, vol. 184, no. 2, pp. 471–483.

KOVAČIĆ, Đ. – KRALIK, D. – RUPČIĆ, S. – JOVIČIĆ, D. – SPAJIĆ, R. – TIŠMA, M. 2017. Soybean straw, corn stover and sunflower stalk as possible substrates for biogas production in Croatia: A review. In Chemical and Biochemical Engineering Quarterly, vol. 31, no. 3, pp. 187–198.

LI, J. – WEI, L. – DUAN, Q. – HU, G. – ZHANG, G. 2014. Semi-continuous anaerobic co-digestion of dairy manure with three crop residues for biogas production. In Bioresource Technology, vol. 156, pp. 307–313.

LI, R. – CHEN, S. – LI, X. 2010. Biogas production from anaerobic co-digestion of food waste with dairy manure in a two-phase digestion system. In Applied Biochemistry and Biotechnology, vol. 160, no. 2, pp. 643–654.

LI, Y. – LI, Y. – ZHANG, D. – LI, G. – LU, J. – LI, S. 2016. Solid state anaerobic co-digestion of tomato residues with dairy manure and corn stover for biogas production. In Bioresource Technology, vol. 217, pp. 50–55.

LI, Y. – PARK, S. Y. – ZHU, J. 2011. Solid-state anaerobic digestion for methane production from organic waste. In Renewable & Sustainable Energy Reviews, vol. 15, pp. 821–826.

LUO, G. – ANGELIDAKI, I. 2013. Co-digestion of manure and whey for in situ biogas upgrading by the addition of H2: process performance and microbial insights. In Applied Microbiology and Biotechnology, vol. 97, no. 3, pp. 1373–1381.

MISHRA, S. – TENNETI, S. 2015. Effect of operational parameters on biogas production using tomato waste as substrate and cow dung as inoculating medium. In International Journal of Scientific Research, vol. 4, no. 5, pp. 148–152.

NGHIEM, L. D. – HAI, F. I. – PRICE, W. E. – WICKHAM, R. – NGO, H. H – GUO, W. 2017. By-products of Anaerobic Treatment: Methane and Digestate from Manures and Cosubstrates. In: Lee, D. – Jegatheesan, V. – Ngo, H. H. – Hallenbeck, P. C. – Pandey, A. editors. Current Developments in Biotechnology and Bioengineering. Amsterdam, London : Elsevier Science B. V., pp. 469 – 473.

OGEJO, J. A. – LI, L. 2010. Enhancing biomethane production from flush dairy manure with turkey processing wastewater. In Applied Energy, vol. 87, no. 10, pp. 3171–3177.

O-THONG, S. – BOE, K. – ANGELIDAKI, I. 2012. Thermophilic anaerobic co-digestion of oil palm empty fruit bunches with palm oil mill effluent for efficient biogas production. In Applied Energy, vol. 93, pp. 648–654.

SAEV, M. – KOUMANOVA, B. – SIMEONOV, I. 2009. Anaerobic co-digestion of wasted tomatoes and cattle dung for biogas production. In Journal of the University of Chemical Technology and Metallurgy, vol. 44, no. 1, pp. 55–60.

SAGHOURI, M. – MANSOORI, Y. – ROHANI, A. – KHODAPARAST, M. H. H. – SHEIKHDAVOODI, M. J. 2018. Modelling and evaluation of anaerobic digestion process of tomato processing wastes for biogas generation. In Journal of Material Cycles and Waste Management, vol. 20, pp. 561–567.

SARADA, R. – JOSEPH, R. 1996. A comparative study of single and two stage processes for methane production from tomato processing waste. In Process Biochemistry, vol. 31, no. 4, pp. 337–340.

SIDDIQ, N. I. – MUNAIM, M. S. A. – ZULARISAM, A. W. 2014. Mesophilic and thermophilic biomethane production by co-digesting pretreated petrochemical wastewater with beef and dairy cattle manure. In Journal of Industrial and Engineering Chemistry, vol. 20, no. 1, pp. 331–337.

SIDDIQUI, Z. – HORAN, N. J. – ANAMAN, K. 2011. Optimisation of C:N ratio for co-digested processed industrial food waste and sewage sludge using the BMP test. In International Journal of Chemical Reactor Engineering, vol. 9, no. 1, note S4.

SIRIPONG, C. – DULYAKASEM, S. 2012. Continuous co-digestion of agro-industrial residues. Master thesis, University of Borås, School of Engineering, Sweden.

TAREKEGN, M. M. – ABEBE, M. A. 2017. Characterization of fruit and vegetable wastes for biogas production under anaerobic condition. In International Journal of Scientific Research and Engineering Studies, vol. 5, no. 1, pp. 0001–0009.

WANG, X. – LU, X. – LI, F. – YANG, G. 2014. Effects of temperature and carbon-nitrogen (C/N) ratio on the performance of anaerobic co-digestion of dairy manure, chicken manure and rice straw: Focusing on ammonia inhibition. In PloS One, vol. 9, no. 5, pp. e97265.

WANG, X. – YANG, G. – FENG, Y. – REN, G. – HAN, X. 2012. Optimizing feeding composition and carbon–nitrogen ratios for improved methane yield during anaerobic co-digestion of dairy, chicken manure and wheat straw. In Bioresource Technology, vol. 120, pp. 78–83.

YUE, Z. – CHEN, R. – YANG, F. – MACLELLAN, J. – MARSH, T. – LIU, Y. – LIAO, W. 2013. Effects of dairy manure and corn stover co-digestion on anaerobic microbes and corresponding digestion performance. In Bioresource Technology, vol. 128, pp. 65–71.

ZARKADAS, I. S. – SOFIKITI, A. S. – VOUDRIAS, E. A. – PILIDIS, G. A. 2015. Thermophilic anaerobic digestion of pasteurised food wastes and dairy cattle manure in batch and large volume laboratory digesters: Focusing on mixing ratios. In Renewable Energy, vol. 80, pp. 432–440.

ZHANG, J. – LOH, K. – LEE, J. – WANG, C. – DAI, Y. – TONG, Y. W. 2017. Three-stage anaerobic co-digestion of food waste and horse manure. In Scientific Reports, vol. 7, pp. 1269.

sciendo

DOI: 10.2478/ata-2019-0008

Acta Technologica Agriculturae 2
Nitra, Slovaca Universitas Agriculturae Nitriae, 2019, pp. 43–47

EVALUATION OF RICE STRAW YIELD, FIBRE COMPOSITION AND COLLECTION UNDER MEDITERRANEAN CONDITIONS

Javier MATÍAS*, Verónica CRUZ, Antonio García, Diana González

Agricultural Research Centre of Extremadura (CICYTEX), Guadajira (Badajoz), Spain

Rice straw remains almost unutilised in the majority of cases and is usually burned. Data on rice residue production under European conditions are extremely limited. A detailed assessment of rice biomass yield, partitioning and straw collection was carried out in Spain. Eleven commercial rice varieties were evaluated in 2015, and two baling trials were performed in 2014 and 2015. The average straw yield was 9.7 t·ha^{-1}. Straw yield, biomass partitioning indices and fibre composition varied significantly according to rice variety. Straw to grain ratio and harvest index were 1.00 and 0.50 on average for rough grain, and 1.25 and 0.41 for husked grain. Biomass partitioning indices significantly correlated with grain yield. Mean content of cellulose, hemicellulose, lignin and ash of rice straw was 32.5%, 19.8%, 6.5% and 13.7%, respectively. Straw amount of less than 3.0 t·ha^{-1} can be collected during the baling trials. Rice straw could represent an eco-friendly source of lignocellulosic biomass in Europe, however, in order to achieve this, baling machine improvements and special crop management should be carried out.

Keywords: agricultural by-products; baling; biomass partitioning; lignocellulosic biomass; greenhouse gases emissions; rice crop

Rice is one of the most widely grown crops in the world. Total area on which the rice is cultivated is approx. 163 million ha; 88% of this cultivation area is located in Asia (Moreno-García et al., 2017). World rice production amounts to approx. 618 million tons per year (Rahimi-Ajdadi et al., 2018). In terms of Europe, majority of rice cultivation areas are located in the Mediterranean countries. Total European harvested area amounts to approx. 642,000 ha and is primarily located in Italy and Spain (Moreno-García et al., 2017). Rice cultivation yields three by-products, straw and the residues after grain milling (husk and bran). Straw and husk remain almost unutilised, despite that various studies have been done in the past. The high mineral content is one of the main limitations to their use as animal feed, apart from its high lignocellulose content (Vadiveloo et al., 2009). Collection of rice straw is still a major challenge. Field baling is by far the least expensive method for harvesting and packing rice straw (Hegazy and Snadro, 2016). Straw collection is complicated because rice is usually grown under waterlogged conditions. In the Mediterranean Basin, rice straw is available for baling in autumn, when weather conditions are not suitable for this operation. On the other hand, the incorporation of rice straw into the paddy soil can cause physiological damage to the crop (Dobermann and Fairhurst, 2000; Olk et al., 2000). For these reasons, rice straw is usually burned, emitting CO_2 into the atmosphere. Burning of rice straw in the open fields results in air pollution, as well as particulate matter release into the atmosphere (Abraham et al., 2016). Nowadays, one of the main world issues is how to reduce the greenhouse gases emissions (GHGe) in order to mitigate the climate change and ensure sustainable economic growth. The EU tries to find cost-efficient ways to make the European economy more climate-friendly. For example, conversion of crop residues can represent one of vital aspects for sustainable development (Abraham et al., 2016). According to the European Commission roadmap, the GHGe should be cut to 40% below the 1990 levels by 2030 and to 80% below the 1990 levels by 2050 (Beloev et al., 2017). Considering all the types of agricultural crop residues, rice straw has been reported to be the most available cellulose source in the world, which makes it interesting for several environmentally friendly applications, like the production of biomaterials, biofuels or high-added value biomolecules (Abraham et al., 2016; Singh et al., 2016). However, accurate quantification of regional scale crop residue represents an essential aspect necessary for designing effective policies and management practices that can contribute toward mitigating GHGe (Fan et al., 2017). Several approaches related to biomass partitioning, like harvest index (*HI*) or straw/grain (*S/G*) ratio, are widely used to estimate the crop residue from data on harvested yield. Nevertheless, data on rice fibrous byproducts production under European conditions are extremely sparse.

Thus, the aim of this work was to conduct a detailed assessment of rice biomass yield and partitioning and collection and fibre composition of straw under Mediterranean conditions.

Material and methods

Experimental field trial

An experimental field trial was carried out during 2015 at the experimental plots of CICYTEX in order to evaluate the straw

Contact address: Javier Matías, Agricultural Research Centre of Extremadura (CICYTEX), 06187 Guadajira (Badajoz), Spain, e-mail: javier.matias@juntaex.es

yield (S) and to determine the biomass partitioning indices (BPI) and straw composition according to their respective variety. Experimental design was a complete randomized blocks with four replications and experimental plot size was 10.0 × 1.5 m. Sowing was conducted in mid-May at a density of 600 seeds per m^2. Average characteristics of the soil at 0–0.6 m depth were: clay loam texture, pH 6.2, 0.87% of organic matter, 88.5 ppm of nitrate, 14.8 ppm of phosphorus and 69.2 ppm of potassium. Eleven commercial rice varieties were evaluated, a hybrid (CLXL745) plus 10 inbred lines. Crop was maintained under flooding. A 200–120–120 kg·ha^{-1} of NPK was applied. In the beginning of October, crop was mowed by hand at ground level and the grain was separated mechanically from the rest of biomass using a thresher.

Baling trials

Two baling trials were conducted on October 30, 2014, and on December 3, 2015, in an open rice field located in the Upper Guadiana River Basin of Extremadura (Southwest Spain). Rice harvest was previously carried out using a combine harvester, distributing the straw in windrows separated at the working width (6.5 m). Plants were cut approx. 0.25 m above the ground level. The variety was Gladio. A lineal metre of straw on the windrows was taken in four randomized points to determine the available straw for baling. The main characteristics of the baling machine (John Deere, 359 model) are 1.42 t of weight, 1.75 m of picker and bales of 0.46 m width and 0.36 m height. A tractor of 82 KW and 5.2 t weight with narrow rubber tires was used. Baling yield (%) was calculated as the baled straw in relation to the available straw for baling. After baling, 5 randomized bales were weighed and measured.

Measurements

Data were expressed on dry weight basis. Dry matter content was determined by drying the samples at 103 ºC over three days. Biomass (B) corresponds to the total aboveground biomass dry matter. Following BPI were used: ratio between straw and grain yield (*S*/*G*) and harvest index (*HI*), which was calculated as the G/B ratio, and is related to *S*/*G* by:

$$HI = 1/(1 + S/G) \quad (1)$$

Rice husk content was determined using a laboratory paddy husker (Satake, Japan). Fibre content and composition (crude fibre, CF; neutral detergent fibre, NDF; acid detergent fibre, ADF and acid detergent lignin, ADL) were analysed following the Ankom procedure. Hemicellulose (H) content was determined by deducting ADF from NDF. Cellulose content (C) was calculated by deducting ADL from ADF. Ash level was measured as the residue remaining after heating at 550 ºC ±10 ºC. Relative Feed Value (RFV) was calculated as Digestible Dry Matter (DDM) multiplied by dry matter intake (DMI as % of Body Weight) and divided by 1.29, where DDM = 88.9 – (0.779 × % ADF) and DMI = 120 / (% NDF).

Statistical analysis

Measured and calculated data were subjected to analysis of variance (ANOVA). In cases when F ratio was significant (P <0.05), Tukey's test was utilized for mean comparison. Linear regression model was used to study relationships between BPI and G. An analysis of covariance (ANCOVA) was performed in order to observe potential influence of variety and yield on BPI, taking variety as factor and yield as covariate. SPSS statistical software was used.

Results and discussion

Experimental field trial

Straw yield and biomass partitioning

Results are shown in Table 1. S and BPI varied significantly on the basis of the respective varieties. The average S was 9.7 t·ha^{-1}. It should be noted that such S is more than two times as much as usually obtained from wheat under Mediterranean conditions (Townsend et al., 2017) and close to that of maize, another summer cereal widely cultivated in Mediterranean regions, at G of 10 t·ha^{-1} (Junta de Extremadura, 2017) and *HI* for maize of 0.50 (Fan et al., 2017; Ion et al., 2015). Different results have been reported for rice in other parts of the world. A higher S (11.8 t·ha^{-1}), but similar G (9.5 t·ha^{-1}), was obtained on average by Osorio et al. (2007), who evaluated 14 rice varieties under tropical conditions. This is consistent with that reported by Hay (1995), who pointed out that G is not correlated with B in rice. In fact, no significant relationship was found between *G* and *S*. Thus, Marquesa variety achieved the highest *G* (10.5 t·ha^{-1}) and the lowest S (8.8 t·ha^{-1}).

The highest B was achieved by the hybrid CLXL 745 (22.2 t·ha^{-1}), which showed relatively low biomass partitioning. This result is not consistent with that reported by several authors who pointed out that hybrid rice have higher G than inbred lines due to a higher partitioning efficiency (Amanullah and Inamullah, 2016; Bueno and Lafarge, 2009). The *S*/*G* ranged from 0.79 to 1.59. Osorio et al. (2007) also determined a significant influence of variety on *S*/*G*, which varied from 0.84 to 2.00. The *HI* varied from 0.39 to 0.56, which is in accordance with results reported for different world places, such as India (Singh et al., 2017), Japan (Hussain et al., 2014), Brazil (Fageria et al., 2011), USA-Florida (Prasad et al., 2006), USA-Texas (Kiniry et al., 2001). Significant relationship (P <0.01) between both BPI and *G* was determined, although less than 30% of the BPI variation could be explained by *G*. However, the ANCOVA result indicated that the variety factor had a significant influence. Taking into account the pairwise comparison of the ANCOVA, if the varieties showing extreme values of both BPI (Gavella and Creso) were not taken into account, relationships were not significantly influenced by variety, and could be more useful for rice crop residue estimation. Results of that linear regression analysis were: S/G = 1.637 - 0.067 G (R^2 = 0.25) and HI = 0.357 + 0.015 G (R^2 = 0.24). It should be noted that this *HI*-*G* relationship is quite similar to that obtained for wheat by Fan et al. (2017). Those BPI were calculated considering rough rice without husk removal, which is very substantial. Average husk content was 19.1%, which is similar to that (20.0%) reported by Hay (1995), and was significantly influenced by variety (Table 1). Therefore, comparison with indices of other crops with bare grains would be inadequate. When husked grain (*G*) was considered, mean harvest index (*HI´*) was 0.41, which

Table 1 Straw yield and biomass partitioning according to variety

Variety	*G* (t·ha^{-1})	*S* (t·ha^{-1})	*S/G*	B (t·ha^{-1})	*HI*	*HI´*	Husk (% G)	Husk (t·ha^{-1})
Gavella	8.1	12.9 a	1.59 a	21.1	0.39 b	0.30 b	21.6 a	1.9
CLX L745	10.2	11.5 ab	1.12 ab	22.2	0.48 ab	0.39 ab	19.1 b	2.1
Mare	10.1	10.3 abc	1.02 b	20.6	0.50 a	0.41 a	18.4 b	1.9
Luna	10.0	9.7 bc	0.97 b	19.6	0.51 a	0.41 a	19.4 b	1.9
Gladio	9.7	9.7 bc	1.00 b	19.4	0.50 a	0.40 a	19.4 b	1.9
Sirio	9.5	9.5 bc	1.00 b	19.0	0.50 a	0.41 a	18.8 b	1.8
Sprint	10.4	9.4 bc	0.90 b	19.8	0.52 a	0.43 a	18.0 b	1.9
Ronaldo	9.5	9.2 bc	0.97 b	18.8	0.51 a	0.41 a	19.1 b	2.0
Marquesa	10.5	8.8 bc	0.83 b	19.3	0.55 a	0.45 a	18.0 b	2.0
Membo	9.2	8.0 c	0.87 b	17.2	0.53 a	0.43 a	18.8 b	1.8
Creso	9.7	7.6 c	0.79 b	17.4	0.56 a	0.45 a	19.7 ab	2.0
Significance	n.s.	***	**	n.s.	**	***	*	n.s.
Mean	9.7	9.7	1.00	19.4	0.50	0.41	19.1	1.9
SEm±	0.8	0.7	0.10	1.13	0.02	0.02	0.4	0.2
HSD	4.2	2.8	0.49	5.8	0.11	0.09	2.1	0.8

G – grain yield (rough grain); *S* – straw yield; B – total biomass yield; *HI* – harvest index for rough grain; *HI´* – harvest index for husked grain; n.s. – no significant difference; means with different letters in the same column differ significantly at * $P = 0.05$, ** $P = 0.01$; *** $P = 0.001$, respectively; SEm ± standard mean error; HSD – critical value for comparison

is in line with results described by Hay (1995), and mean *S/G´* was 1.25. Correlation with the corrected grain yield (G´) was also significant in both cases, with similar regression coefficients. Considering both types of fibrous byproducts (straw + husk), the average yield was 11.6 t·ha^{-1}, ranging significantly according to variety. An average of 1.20 t of fibrous byproducts per tonne of grain was determined, which is in compliance with results observed by Matsumura et al. (2005).

Fibre content and composition, ash content and relative feed value (RFV) of rice straw according to variety

Results are shown in Table 2. Variety had significant influence on fibre content and composition, which is in line with that reported by others (Sarnklong et al., 2010; Vadiveloo and Phang, 1996). Fibre content and composition correlated neither with S nor with BPI.

CF, NDF, ADF, ADL, C and H were lower than those reported by Fedna (2013) for wheat and barley straw (36.0%, 72.0%, 46.4%, 8.4%, 38.0%, 25.6%), the most abundant crop byproducts in Spain (Palumbo et al., 2015), which is in line with that quoted by Bakker et al. (2013). Nevertheless, potential yield of cellulose from rice straw (mean of 3.2 t·ha^{-1}, with significant differences among varieties) is quite higher than from winter cereals straw (1.5 t·ha^{-1}), considering a straw yield of 4.0 t·ha^{-1} for wheat and barley (Townsend et al., 2017). Furthermore, approx. 0.5 t·ha^{-1} of cellulose could be also obtained from rice husk, taking into account the average husk yield (1.9 t·ha^{-1}) and 35.6% of cellulose (Matías et al., 2018). Cellulose content of rice straw was quite lower than that (41–57%) stated by Liu et al. (2013) and similar to that reported by others (Bakker et al., 2013; Sarnklong et al., 2010; Abou-El-Enin et al., 1999; Vadiveloo and Phang, 1996). Hemicellulose content was quite lower than that reported by others (Liu et al., 2013, Bakker et al., 2013; Sarnklong et al., 2010; Abou-El-Enin et al., 1999; Vadiveloo and Phang, 1996). Lignin content showed values in line with those determined by Vadilevo and Phang (1996), but lower than those quoted in some papers (Hasanjanzadeha et al., 2014; Liu et al., 2013; Bakker et al., 2013) and slightly higher than the average value calculated by Abou-El-Enin et al. (1999). High lignocellulosic content in rice straw has been reported to be a limitation for its feeding use by Vadiveloo et al. (2009). However, average lignocellulosic content in rice straw in this work (58.8%) was lower than that reported for wheat and barley straw (72.0%) by Fedna (2013). On the contrary, average ash content in rice straw (13.7%) was higher than that stated by Fedna (2013) for winter cereals (7.2%). Ash content varied significantly from 12.0% to 16.1%, which are in reasonable agreement with values reported by others (Hasanjanzadeha et al., 2014; Bakker et al., 2013; Sarnklong et al., 2010; Vadiveloo, 2000; Vadiveloo and Phang, 1996). RFV values varied significantly among varieties and were higher than those (61.0–68.0) stated by Fekadu et al. (2017) and calculated for wheat and barley straw (68.2) by Fedna (2013). Varietal differences in the nutritional value of rice straw were also reported by Vadiveloo and Phang (1996). In principle, the higher the RFV, the better the quality for feeding uses. However, high ash content in rice straw and its high silica content highly reduce its nutritional value (Vadiveloo et al., 2009).

Baling trials

The results were 2.9 t·ha^{-1} (2014) and 2.0 t·ha^{-1} (2015) of baled straw. Differences between years can be explained because, in 2015, the baling operation was delayed until December due to intense rainfall occurring from September to November (161.7 mm), most likely resulting in straw

Table 2 Fibre content and composition, ash content and relative feed value (RFV) of rice straw according to variety

Variety	CF (%)	Ash (%)	NDF (%)	ADF (%)	ADL (%)	RFV	C (%)	H (%)
Marquesa	31.3 a	14.7 ab	60.7 ab	40.2 ab	5.7 ab	88.4 ab	33.9 abc	20.5 a
Mare	30.5 ab	13.8 abc	62.0 a	42.1 a	6.8 ab	84.2 b	35.3 ab	19.9 ab
Sprint	30.5 ab	13.2 bc	61.6 a	40.3 ab	6.4 ab	87.0 ab	34.0 abc	21.2 a
CLX L745	30.3 ab	16.1 a	60.1 ab	41.7 a	6.4 ab	87.6 ab	36.0 a	18.5 ab
Creso	28.5 ab	14.3 abc	57.8 ab	39.2 ab	6.9 ab	94.4 ab	32.3 abc	18.6 ab
Gladio	27.7 ab	12.6 bc	59.3 ab	38.8 ab	6.6 ab	92.2 ab	32.3 abc	20.4 ab
Ronaldo	27.4 b	13.2 bc	57.9 ab	37.8 ab	6.4 ab	95.6 ab	31.4 bc	20.1 ab
Gavella	27.3 b	12.0 c	58.1 ab	36.1 b	5.2 b	97.4 ab	31.0 c	21.9 a
Membo	27.0 b	14.4 ab	55.0 b	38.2 ab	7.3 a	100.5 a	31.0 c	16.8 b
Luna	26.9 b	12.8 bc	56.7 ab	38.2 ab	7.4 a	97.4 ab	31.0 c	18.6 ab
Sirio	26.9 b	13.9 abc	57.6 ab	36.4 b	6.3 ab	97.9 ab	30.1 c	21.1 a
Significance	***	***	**	***	**	**	***	***
Mean	28.6	13.7	58.0	39.0	6.5	92.9	32.5	19.8
SEm±	0.76	0.48	1.17	0.92	0.38	2.89	0.81	0.74
HSD	3.75	2.38	5.76	4.54	1.85	14.2	3.97	3.65

CF – crude fibre; NDF – neutral detergent fibre; ADF – acid detergent fibre; ADL – lignin acid detergent; RFV – relative feed value; C – cellulose; H – hemicellulose; means with different letters in the same column differ significantly at ** $P = 0.01$;*** $P = 0.001$; SEm ± standard mean error; HSD – critical value for comparison

loss. These results are lower than those (approx. 4 t·ha^{-1}) reported for winter cereals (Garstang et al., 2009). Average characteristics of the bales (weight, humidity content and density on fresh basis) were (in 2014–2015): 18.8–19.5 kg, 21.0–21.3% and 117.9–127.1 kg·m-3. The baled yields (62% in 2014 and 68% in 2015) were lower than the available straw for baling (4.9 t·ha^{-1} in 2014 and 2.9 t·ha^{-1} in 2015). Straw losses during the baling operation could be due to several reasons. Despite the low tractor speed (approx. 1.5 km·h-1), the high amount of straw on the windrows with relatively high moisture content (around 25%) saturated the bale-chamber. Nevertheless, according to Singh et al. (2016), the moisture level was relatively good for baling in terms of adverse conditions. On the other hand, straw losses probably also occurred during the pick-up step due to relatively high moisture content. Available straw amount for baling was quite lower than the straw yield, but it should be noted that rice is usually cut relatively high due to flooding conditions of rice fields. In order to increase the baled straw yield of rice crop, some modifications in baler machine should be developed, such as higher feeding and compression capacity. Furthermore, a special crop management should be carried out to favour an earlier harvest for avoiding autumn rains, trying to harvest at a higher height.

Conclusions

Rice crop has high straw yield under Mediterranean conditions, approx. 10 t·ha^{-1}, with significant differences among varieties. Individual varieties showed significant impacts on majority of evaluated parameters, which makes estimations based on average rice crop values less accurate. Significant relationships (P <0.01) were observed between both BPI and G, but these should be taken into account with caution, because less than 30% of the BPI variation could be explained by G. New works should be carried out to confirm the stability of those relationships between varieties. Straw fibre content and composition were influenced neither by S nor by G. The RFV was relatively good (92.9), although average ash content was high (13.7%). Rice straw showed to be a good eco-friendly source of lignocellulosic biomass in Europe, with approx. 32.5% of cellulose. More than 3.0 t·ha^{-1} of cellulose could be potentially obtained from rice straw. Nevertheless, results of straw collection were low. Less than 3.0 t·ha^{-1} could be baled. To increase the amount of baled straw, a special crop management should be carried out and improvements in baling machine should be developed.

Acknowledgements

This work was supported by the WALEVA LIFE + project (LIFE13 ENV/ES/001165). The authors are grateful to Don Benito Farmers Association (Spain) for their helpful cooperation.

References

ABOU-EL-ENIN, O. H. – FADE, J. G. – MACKILL, D. J. 1999. Differences in chemical composition and fibre digestion of rice straw with, and without, anhydrous ammonia from 53 rice varieties. In Animal Feed Science and Technology, vol. 79, pp. 129–136.

ABRAHAM, A. – MATHEW, A. K. – SINDHU, R. – PANDEY, A. – BINOD, P. 2016. Potential of rice straw for bio-refining: An overview. In Bioresource Technology, vol. 215, pp. 29–36.

AMANULLAH, J. – INAMULLAH, Z. 2016. Dry matter partitioning and harvest index differ in rice genotypes with variable rates of phosphorus and zinc nutrition. In Rice Science, vol. 23, no. 2, pp. 78–87.

BAKKER, R. R. C. – ELBERSEN, H. W. – POPPENS, R. P. – LESSCHEN, J. P. 2013. Rice straw and wheat straw. Potential feedstocks for the biobased economy. Netherlands Agency.

BELOEV, I. – GABROVSKA-EVSTATIEVA, K. – EVSTATIEV, B. 2017. Compensation of CO_2 emissions from petrol stations with photovoltaic parks: Cost-benefit and risk analysis. In Acta Technologica Agriculturae, vol. 20, no. 4, pp. 85–90.

BUENO, C. S. – LAFARGE, T. 2009. Higher crop performance of rice hybrids than of elite inbreds in the tropics: 1. Hybrids accumulate more biomass during each phenological phase. In Field Crops Research, vol. 112, pp. 229–237.

DOBERMANN, A. – FAIRHURST, T. H. 2000. Chapter 1.9. Managing Organic Manures, Straw, and Green Manure. In Rice: Nutrient disorders & nutrient management. Handbook series. Potash & Phosphate Institute (PPI), Potash & Phosphate Institute of Canada (PPIC) and International Rice Research Institute (IRRI), pp. 38–42. ISBN 9789810579494.

FAN, J. – McCONKEY, B. – JANZEN, H. – TOWNLEY-SMITH, L. – WANG, H. 2017. Harvest index–yield relationship for estimating crop residue in cold continental climates. In Field Crops Research, vol. 204, pp. 153–157.

FAGERIA, N. K. – MOREIRA, A. – COELHO, A. M. 2011. Yield and yield components of upland rice as influenced by nitrogen sources. In Journal of Plant Nutrition, vol. 34, pp. 361–370.

FEDNA. 2013. FEDNA – Spanish Foundation for the Development of Animal Nutrition – standards for the formulation of compound feed (Normas Fedna – Fundación Española para el Desarrollo de la Nutrición Animal – para la formulación de piensos compuestos).

FEKADU, D. – WALELEGN, M. – TEREFE, G. 2017. Indexing Ethiopian feed stuffs using relative feed value: Dry forages and roughages, energy supplements, and protein supplements. In Journal of Biology, Agriculture and Healthcare, vol. 7, no. 21, pp. 57–60.

GARSTANG, J. – MACKIE, E. – MATTHEWS, R. – PROCTER, C. H. – RANDLE, T. – SMITH, C. – TUBBY, I. – WILSON, L. 2009. Bioenergy Review – Mapping Work. Science report: SC070001/SR2. Environment Agency.

HASANJANZADEHA, H. – HEDJAZIA, S. – ASHORIB, A. – MAHDAVIC, S. – YOUSEFI, H. 2014. Effects of hemicellulose pre-extraction and cellulose nanofiber on the properties of rice straw pulp. In International Journal of Biological Macromolecules, vol. 68, pp. 198–204.

HAY, R. K. M.1995. Harvest index: A review of its use in plant breeding and crop physiology. In Annals of Applied Biology, vol. 26, pp. 197–216.

HEGAZY, R. – SNADRO, J. M. 2016. Rice straw collection. International Rice Research Institute Crop and Environmental Sciences Division Postharvest Unit.

HUSSAIN, S. – FUJII, T. – MCGOEY, S. – YAMADA, M. – RAMZAN, M. – AKMAL, M. 2014. Evaluation of different rice varieties for growth and yield characteristics. In Journal of Animal and Plant Sciences, vol. 24, no. 5, pp. 1504–1510.

ION, V. – DICU, G. – DUMBRAVĂ, M. – TEMOCICO, G. – ALECU, I. N. – BĂŞA, A. G. – STATE, D. 2015. Harvest index at maize in different growing conditions. In Romanian Biotechnological Letters, vol. 20, no. 6, pp. 1–10.

JUNTA DE EXTREMADURA. 2017. Agriculture and livestock of Extremadura in 2016 (La agricultura y la ganadería extremeñas 2016). Fundación CB. 364 pp.

KINIRY, J. R. – MC-CAULEY, G. – XIE, Y. – ARNOLD, J. G. 2001. Rice parameters describing crop performance of four rice cultivars. In Agronomy Journal, vol. 93, pp. 1354–1361.

LIU, Z. – LIU, X. – FEI, B. – JIANG, Z. – CAI, Z. – YUA, Y. 2013. The properties of pellets from mixing bamboo and rice straw. In Renewable Energy, vol. 55, pp. 1–5.

MATÍAS, J. – GARCÍA, A. – GONZÁLEZ, D. – GARCÍA, J. – HERNÁNDEZ-GARCÍA, F. I. – IZQUIERDO, M. 2018. Use of rice husk in Iberian pigs during the pre-montanera period for welfare diets. Preliminary results. In Archivos de Zootecnia, Proceedings 9th International Symposium on the Mediterranean Pig, Portalegre (Portugal), pp. 37–40.

MATSUMURA, Y. – MINOWAB, T. – YAMAMOTO, H. 2005. Amount, availability, and potential use of rice straw (agricultural residue) biomass as an energy resource in Japan. In Biomass and Bioenergy, vol. 29, pp. 347–354.

MORENO-GARCÍA, B. – GUILLÉN, M. – QUÍLEZ, D. 2017. Response of paddy rice to fertilisation with pig slurry in northeast Spain: Strategies to optimise nitrogen use efficiency. In Field Crops Research, vol. 208, pp. 44–54.

OLK, D. C. – VAN KESSEL, C. – BRONSON, K. F. 2000. Managing soil organic matter in rice and non-rice soils: Agronomic questions. In Carbon and Nitrogen Dynamics in Flooded Soils. International Rice Research Institute, Los Baños, Philippines, pp. 27–47. ISBN 9712201406.

OSORIO, J. F. 2007. Evolution of growth, grain yield and partition of photosynthates in 14 varieties of rice representing various breeding cycles in Colombi. Universidad de Colombia, Palmira. 135 pp. (In Spanish: Evolución del crecimiento, rendimiento de grano y partición de fotosintatos en 14 variedades de arroz representantes de diversos ciclos de mejoramiento en Colombia).

PALUMBO, M. – AVELLANEDA, J. – LACASTA, A. M. 2015.Availability of crop by-products in Spain: New raw materials for natural thermal insulation. In Resources, Conservation and Recycling, vol. 99, pp. 1–6.

PRASAD, P. V. V. – BOOTE, K. J. – ALLEN, L. H – SHEEHY, J. E. – THOMAS, J. M. G. 2006. Species, ecotype and cultivar differences in spikelet fertility and harvest index of rice in response to high temperature stress. In Field Crops Research, vol. 95, pp. 398–411.

RAHIMI-AJDADI, F. – ASLI-ARDEH, A. A. E. – AHMADI-ARA, A. 2018. Effect of varying parboiling conditions on head rice yield for common paddy varieties in Iran. In Acta Technologica Agriculturae, vol. 21, no. 1, pp. 1–7.

SARNKLONG, C. – CONE, J. W. – PELLIKAAN, W. – HENDRIKS, W. H. 2010. Utilization of rice straw and different treatments to improve its feed value for ruminants: A review. In Asian-Australasian Journal of Animal Science, vol. 23, no. 5, pp. 680–692.

SINGH, D. K – GUPTA, S. – NANDA, G. – SHARMA, Y. – SINGH, V. V. – BISARYA, D. 2017. Evaluation of rice varieties for yield under organic farming in Tarai. In International Journal of Current Microbiology and Applied Science, vol. 6, no. 4, pp. 734–738.

SINGH, R. – SRIVASTAVA, M. – SHUKLA, A. 2016. Environmental sustainability of bioethanol production from rice straw in India: A review. In Renewable and Sustainable Energy Reviews, vol. 54, pp. 202–216.

TOWNSEND, T. J. – SPARKES, D. L. – WILSON, P. 2017. Food and bioenergy: Reviewing the potential of dual purpose wheat crops. In GCB Bioenergy, vol. 9, pp. 525–540.

VADIVELOO, J. – NURFARIZA, B. – FADEL, J. G. 2009. Nutritional improvement of rice husks. In Animal Feed Science and Technology, vol. 151, no. 3, pp. 299–305.

VADIVELOO, J. 2000. Nutritional properties of the leaf and stem of rice straw. In Animal Feed Science and Technology, vol. 83, pp. 57–65.

VADIVELOO, J. – PHANG, O. C. 1996. Differences in the nutritive value of two rice varieties as influenced by season and location. In Animal Feed Science and Technology, vol. 61, pp. 247–258.

sciendo

DOI: 10.2478/ata-2019-0009

Acta Technologica Agriculturae 2
Nitra, Slovaca Universitas Agriculturae Nitriae, 2019, pp. 48–55

COMPARISON OF PVD COATINGS NACRO[4] AND TIALN + DLC DEPOSITED ON HIGH CONTACT RATIO GEARING INTERACTING WITH CONVENTIONAL AND ECOLOGICAL LUBRICANTS

Adam FÜRSTENZELLER[1]*, František TÓTH[1], Milan KADNÁR[1], Juraj RUSNÁK[1], Miroslav BOŠANSKÝ[2]

[1]Slovak University of Agriculture in Nitra, Slovakia
[2]Slovak University of Technology in Bratislava, Slovakia

Proposed paper deals with experimental tests performed on the Nieman M01 FZG test rig. Experiments were carried out in accordance with STN 65 6280 standard for FZG scuffing tests, from which load values for each load level were obtained. HCR gears made of 16MnCr5 material were utilized during experimental tests. Gear surface was deposited by PVD coatings of nACRo[4] and TiAlN + DLC. Conventional lubricant MADIT PP 90H and biological lubricant OMW Biogear S150 were selected for lubrication environments. Aim of the experimental tests lied in application and comparison of PVD coatings deposited on HCR gears. Values of the maximum height of the assessed profile *Rz* for tip and reference diameters were measured after each load level. Results of experimental tests were statistically processed and relations between the maximum height of assessed profile *Rz* and load levels for both utilized coatings in both environments were established on the basis of these results.

Keywords: HCR gearing; PVD coating nACRo[4]; PVD coating TiAlN + DLC; FZG scuffing test; ecological oil introduction

Gears and power transmissions are the oldest mechanisms used in engineering. They were used whenever a man wanted to transfer mechanical energy to a working machine. Gears have undergone a long way of development to current state-of-the-art form of technology (Hoehn et al., 2008; Rackov et al., 2014; Kadnár et al., 2017).

High Contact Ratio (HCR) gears are non-standard gears with a modified form of a basic involute profile (Bošanský et al., 2013a). Changes are related to addendum height; it does not equal 1 like standard involute gears. Addendum height h_a* increases and exceeds 1 (h_a* >1). Such gears have contact ratio $\varepsilon_\alpha \geq 2$. Teeth with this profile can reach contact ratio up to 4 (Tulík et al., 2017; Tulík et al., 2013; Máchal et al., 2013).

Principle of physical vapour deposition (PVD) lies in conversion of deposited material to the gas phase (evaporation, sputtering) in a vacuum, followed by application to a substrate at low temperatures (150–500 °C) (Lümkemann et al., 2014). Coating material or its components must be present directly in the deposition chamber, in which they are transferred to gaseous state. Typical layer thickness ranges from 1–5 µm (Hatamleh et al., 2009; Bošanský et al., 2013b; Dostál et al., 2019).

The PVD coating method was utilized for experimental study in order to ensure more appropriate temperature course during coating and lower procurement costs. Other method of coating with higher deposition temperatures was not utilized, since gears were surface-hardened and deposition temperature would exceed quench temperature (Bobzin et al., 2009). After considering these factors and options in cooperation with the LISS CZ company, it was decided to use PVD coatings. Coating production was carried out in laboratories of LISS and selected coatings were deposited by means of the ARC PVD using device π411PLUS. Parameters of coatings used are described in the chapter Materials and Methods.

Material and methods

Experimental tests were performed at the Center of Innovation laboratories at the Faculty of Mechanical Engineering, Slovak University of Technology in Bratislava. Experiment was performed in accordance with STN 65 6280 standard for FZG (Forschungsstelle für Zahnräder und Getriebebau – Gear Research Centre) scuffing tests, from which the load values for different load levels were obtained (STN 656280, 1985). Experiment was performed using the FZG test rig (back-to-back) with closed performance flow, portable surface roughness tester Mitutoyo SJ-201 and ultrasonic cleaner Ecosom U7-STH (Bromark et al., 1992; Pengbo et al., 2017).

Niemann M01 device was developed at laboratories of the Slovak University of Technology in Bratislava for the comprehensive measurement of scuffing tests. Niemann M01 gear test rig is a back-to-back rig (Fig. 1).
The device itself is complemented by a number of devices for tracking of measured data during machine operation.

Contact address: Adam Fürstenzeller, Slovak University of Agriculture in Nitra, Faculty of Engineering, Department of Machine Design, Tr. Andreja Hlinku 2, 949 76 Nitra, Slovakia, e-mail: xfurstenzell@is.uniag.sk

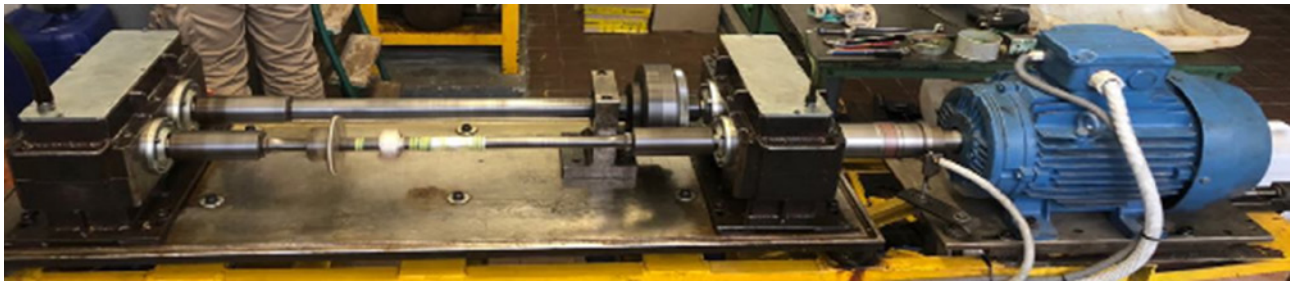

Fig. 1 Niemann M01 FZG back-to-back test rig

These devices serve as feedback to the data set before the measurement (Michalczewski et al., 2013).

Utilized lubricants for experimental tests included OMV BioGear S 150 and MADIT PP90H. The reason for using of biological and conventional lubricants was to test the durability and resistance of coating in selected lubricants under extreme conditions. Furthermore, specific types of lubricant – OMV Biogear S150 and MADIT PP 90H – were used since these were previously observed in experiments at the Center of Innovation, making it possible to compare them with previous research (Bošanský et al., 2012; Bošanský and Rusnák, 2017).

OMV Biogear S 150 is fully synthetic, biodegradable, industrial gear oil based on synthetic environment-friendly esters; basic specifications of this device are shown in Table 1. It is designed for mechanically and thermally heavy load transmissions of various constructions, for bearing lubrication in agriculture, forestry, construction industry, shipping and protcted natural areas.

Table 1 Technical properties of OMV Biohyd S 150 oil

Property	Value
Viscosity at 40 °C	150.00 $mm^2 \cdot s^{-1}$
Viscosity at 100 °C	24.45 $mm^2 \cdot s^{-1}$
Ignition point	224 °C
Pour point	-27 °C
Density at 15 °C	945 $kg \cdot m^{-3}$
Viscosity index	167

MADIT PP 90H is a year-round transmission oil designed to lubricate extremely heavy-duty transmissions and final-drive assemblies of modern cars and other mobile technology. Its basic specification is shown in Table 2.

Table 2 Technical data of MADIT PP 90H

Property	Value
Viscosity at 40 °C	140.00 $mm^2 \cdot s^{-1}$
Viscosity at 100 °C	15.00 $mm^2 \cdot s^{-1}$
Ignition point	200 °C
Pour point	-27 °C
Density at 15 °C	905 $kg \cdot m^{-3}$
Viscosity index	95

It is suitable for gearboxes working under extremely demanding operating conditions. It is designed for hypoid transmissions and is preferred in case of elevated temperatures, ensuring reliable function.

Portable surface roughness tester Mitutoyo SJ-201 with a retrofitted measuring apparatus was used for measuring of roughness before loading and after each load stage. The device was installed on the apparatus and used for measurement of the maximum height of assessed profile *Rz* on tip and reference diameter on both pinion and gear. Pinion and gear were degreased, washed in technical gasoline, cleaned from oil residues in an ultrasonic cleaner and dried with a flow of air before each measurement.

Test gears were made of 16MnCr5 steel and carburized, case hardened and tempered before coating. Basic parameters, such as the number of teeth of pinion and gear, are shown in Table 3.

Table 3 Main parameters of test HCR gears

Property	Value
Transmission ratio	$i = 2.43$
Centre distance	$a = 144$ mm
Module	$m = 4$ mm
Number of teeth – pinion – gear	$z_1 = 21$ $z_2 = 51$
Face width	$b = 15$ mm
Reference cylinder helix angle	$\beta = 0$ °
Reference pressure angle	$\alpha = 20$ °
Addendum	$h_a^* = 1.3$
Dedendum	$h_f^* = 1.7$
Profile shift correction – pinion – gear	$x_1 = 0.4$ $x_2 = -0.4$
Tip diameter – pinion – gear	$d_{a_1} = 97.6$ mm $d_{a_2} = 2$ mm
Traverse contact ratio	$\varepsilon_\alpha = 2.003$

For the experimental tests, PVD coatings nACRo[4] and TiAlN + DLC were selected, the properties of which are shown in Table 4. Selected coatings are manufactured with a thickness ranging from 1 to 7 µm. The coating thickness of 7 µm was utilized in experiment according to the standard.

Experimental tests for each coating were performed in 2 phases. In the first phase, experiments were carried out with OMV Biogear S150 ecological lubricant and with

Table 4 Properties of nACRo^4 and TiAlN + DLC coatings

Property	nACRo^4	TiAlN + DLC
Colour	Grey	Violet-black
Nanohardness up to	40 GPa	36 GPa
Thickness	1–7 µm	1–7 µm
Friction coefficient	0.45	0.60
Maximum usage temperature	1,100 °C	700 °C
Deposition temperature	480 °C	480 °C

conventional lubricant MADIT PP 90H in the second phase. After completion of both phases, testing of another coating was carried out.

Preparation of the test

To avoid errors and inaccuracies, several steps had to be taken before each test in order to prepare the device and test gears:

- cleaning the chambers twice with a suitable solvent before starting a new series of experiments with a different lubricant;
- cleaning the pinion and gear in a solvent;
- weighing the pinion and gear on scale with an accuracy of at least 1 mg.

Conditions of experiment were determined by standard STN 65 6280:

- required circumferential velocity on the pinion – v = 6.4 m·s^{-1}, corresponding to the pinion revolutions of 1,450 rpm in this case;
- test duration for each load stage – 20.6 min, showing that the test pinion has performed 30,000 cycles (STN 656280, 1985).

Expected procedure for the experiment:

- insertion of testing gears into the test chamber, pouring of oil into chamber and assembling the measuring device;
- loading the test gears with the torque according to standard;
- launching the device for 20.6 min.;
- draining used oil;
- demounting the test chamber and removal of the test gear;
- degreasing the gears, washing the gears in technical gasoline and cleaning from oil residues in the ultrasonic cleaner, drying gears with the flow of dry air,
- weighing gears and measuring roughness.

Results and discussion

Experimental tests were performed on HCR gears, coated with nACRo^4 and TiAlN + DLC coatings in accordance with STN 65 6280 standard for FZG scuffing tests utilizing the Nieman M01 testing rig. Conventional lubricant MADIT PP 90H and ecological lubricant OMW Biogear S150 were selected for lubrication purposes. Results obtained from experimental tests were statistically processed and assessed. Test results were graphically evaluated as the course of the maximum height of the assessed profile *Rz* depending on the load level. Increasing load level was followed by a gradual increase of the *Rz* values caused by abrasion of the coating layers. When the value of the *Rz* would reach a limit 7 µm, this load level is marked as a border level of load.

Table 5 Values of the maximum height of the assessed profile *Rz* (pinion, nACRo^4, Biogear S150)

Load level	Tip diameter				Reference diameter			
	n	*R´z* (µm)	*S* (µm)	$S_{R´z}$ (µm)	*n*	*R´z* (µm)	*S* (µm)	$S_{R´z}$ (µm)
3	10	5.600	0.189	0.059	10	3.65	0.092	0.029
4	10	6.080	0.077	0.024	10	4.68	0.204	0.064
5	10	5.670	0.061	0.019	10	3.11	0.086	0.027
6	10	5.030	0.089	0.028	10	1.36	0.077	0.024
7	10	3.760	0.165	0.052	10	1.20	0.074	0.023
7.5	10	5.070	0.075	0.023	10	1.44	0.094	0.029
8	10	5.460	0.085	0.027	10	1.85	0.079	0.025
9	10	5.380	0.076	0.024	10	1.89	0.072	0.023
10	10	2.770	0.092	0.029	10	1.24	0.044	0.014
11	10	3.310	0.089	0.028	10	1.09	0.067	0.021
12	10	2.700	0.154	0.049	10	1.40	0.076	0.024

Table 6 Values of maximum height of the assessed profile *Rz* (gear, nACRo[4], Biogear S150)

Load level	Tip diameter				Reference diameter			
	n	*R´z* (µm)	*S* (µm)	$S_{R´z}$ (µm)	*n*	*R´z* (µm)	*S* (µm)	$S_{R´z}$ (µm)
3	10	5.890	0.094	0.030	10	3.61	0.110	0.035
4	10	6.530	0.041	0.013	10	6.59	0.112	0.039
5	10	5.880	0.056	0.018	10	4.48	0.107	0.034
6	10	5.940	0.108	0.034	10	4.94	0.133	0.042
7	10	5.410	0.069	0.022	10	4.14	0.117	0.037
7.5	10	6.480	0.105	0.033	10	3.78	0.164	0.052
8	10	6.360	0.098	0.031	10	4.68	0.154	0.049
9	10	5.820	0.092	0.029	10	3.46	0.175	0.055
10	10	5.640	0.104	0.033	10	4.07	0.133	0.042
11	10	5.470	0.133	0.042	10	2.70	0.193	0.061
12	10	5.150	0.112	0.035	10	2.70	0.198	0.063

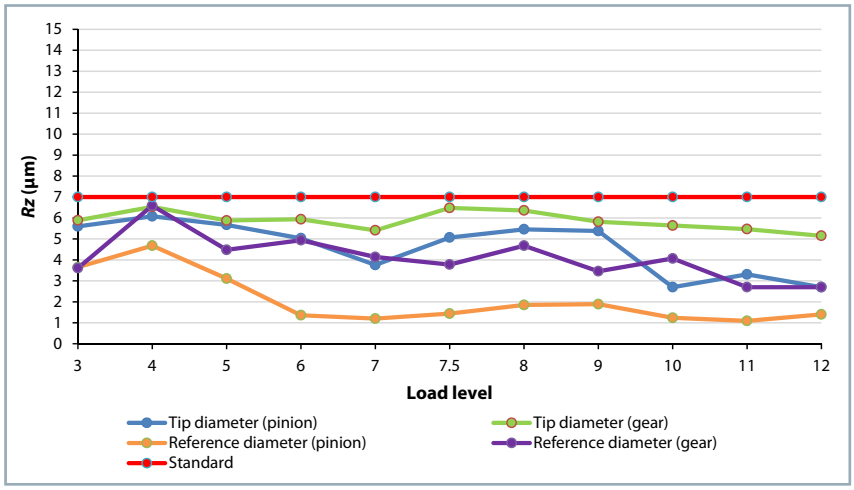

Fig. 2 Dependence of change maximum height of the assessed profile *Rz* on load level for nACRo[4] in OMV Biogear S 150

Fig. 2 shows a change in the maximum height of the assessed profile *Rz* depending on the load level for both pinion and gear. Gear pair was coated by PVD coating nACRo[4] and lubricated with biological oil OMW Biogear S150. There are 5 lines in graph showing reference and tip diameters for the pinion and gear and limit value of the maximum height of the assessed profile *Rz* defined by the standard. These lines are colour-coded for better clarity. Tables 5 and 6 show that the maximum value of assessed profile *Rz* did not reach a limit value of 7 µm.

Fig. 3 shows a change in the maximum height of the assessed profile *Rz* depending on load level

Table 7 Values of the maximum height of the assessed profile *Rz* (pinion, nACRo[4], MADIT PP90H)

Load level	Tip diameter				Reference diameter			
	n	*R´z* (µm)	*S* (µm)	$S_{R´z}$ (µm)	*n*	*R´z* (µm)	*S* (µm)	$S_{R´z}$ (µm)
3	10	4.140	0.105	0.033	10	3.910	0.096	0.030
4	10	5.310	0.156	0.049	10	4.010	0.163	0.052
5	10	4.610	0.191	0.060	10	1.890	0.124	0.039
6	10	4.010	0.144	0.045	10	2.520	0.132	0.042
7	10	4.570	0.136	0.043	10	2.240	0.099	0.031
7.5	10	3.550	0.137	0.043	10	4.180	0.130	0.983
8	10	4.260	0.126	0.040	10	1.950	0.119	0.038
9	10	4.640	0.155	0.049	10	1.340	0.150	0.048
10	10	4.770	0.131	0.041	10	1.530	0.112	0.035
11	10	5.180	0.128	0.040	10	1.660	0.123	0.038
12	10	4.920	0.082	0.026	10	1.720	0.119	0.038

Table 8 Values of the maximum height of the assessed profile *Rz* (gear, nACRo[4], MADIT PP90H)

Load level	Tip diameter				Reference diameter			
	n	*R'z* (µm)	*S* (µm)	$S_{R'z}$ (µm)	*n*	*R'z* (µm)	*S* (µm)	$S_{R'z}$ (µm)
3	10	6.040	0.131	0.041	10	5.030	0.114	0.036
4	10	5.510	0.159	0.050	10	5.010	0.144	0.046
5	10	5.510	0.147	0.047	10	4.260	0.103	0.033
6	10	6.670	0.131	0.042	10	4.240	0.138	0.044
7	10	4.890	0.121	0.038	10	5.560	0.120	0.038
7.5	10	5.530	0.104	0.033	10	4.520	0.114	0.036
8	10	5.810	0.129	0.041	10	2.210	0.115	0.036
9	10	4.990	0.126	0.040	10	3.880	0.121	0.038
10	10	5.840	0.174	0.055	10	1.510	0.141	0.044
11	10	4.810	0.102	0.032	10	2.850	0.122	0.039
12	10	5.370	0.148	0.047	10	3.090	0.110	0.035

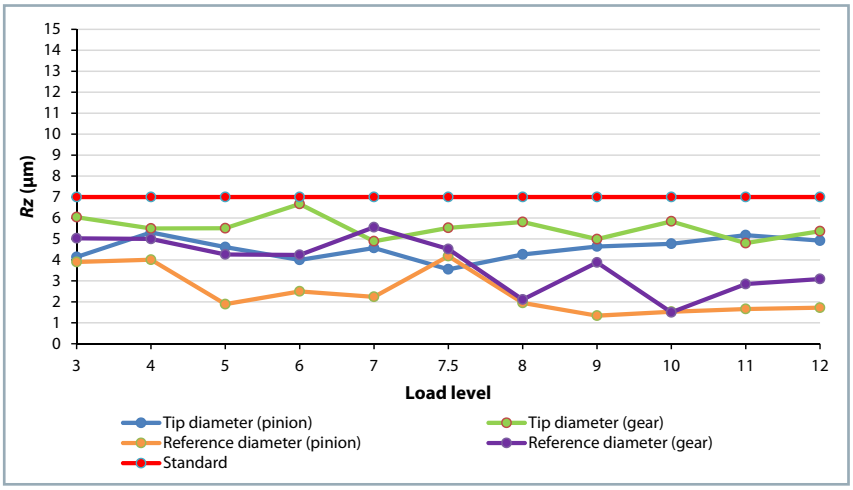

Fig. 3 Dependence of change in the maximum height of the assessed profile *Rz* on load level for nACRo[4] in MADIT PP 90H

for both pinion and gear. Gear pair was coated by PVD coating nACRo[4] and lubricated with conventional oil MADIT PP 90H. There are 5 lines in the graph showing the reference and tip diameters for the pinion and gear and limit value of the maximum height of the assessed profile *Rz* defined by the standard. These lines are colour-coded for better clarity. Tables 7 and 8 show that the maximum value of the assessed profile *Rz* did not reach a limit value of 7 µm.

Fig. 4 shows a change in the maximum height of the assessed profile *Rz* depending on load level for both pinion and gear. Gear pair was coated by PVD coating TiAlN + DLC and

Table 9 Values of the maximum height of the assessed profile *Rz* (pinion, TiAlN + DLC, Biogear S150)

Load level	Tip diameter				Reference diameter			
	n	*R'z* (µm)	*S* (µm)	$S_{R'z}$ (µm)	*n*	*R'z* (µm)	*S* (µm)	$S_{R'z}$ (µm)
3	10	6.920	0.137	0.043	10	6.410	0.113	0.036
4	10	5.760	0.127	0.040	10	4.710	0.098	0.031
5	10	6.210	0.134	0.042	10	5.070	0.144	0.036
6	10	4.910	0.176	0.056	10	5.350	0.130	0.033
7	10	5.030	0.160	0.034	10	4.360	0.121	0.038
7.5	10	4.830	0.139	0.044	10	5.890	0.114	0.036
8	10	6.340	0.128	0.041	10	3.970	0.134	0.042
9	10	4.840	0.117	0.037	10	2.710	0.123	0.039
10	10	5.790	0.145	0.046	10	2.870	0.136	0.043
11	10	5.780	0.145	0.046	10	3.940	0.104	0.033
12	10	5.080	0.128	0.040	10	2.240	0.096	0.030

Table 10 Values of the maximum height of the assessed profile *Rz* (gear, TiAlN+DLC, Biogear S150)

Load level	Tip diameter				Reference diameter			
	n	*R'z* (µm)	*S* (µm)	$S_{R'z}$ (µm)	*n*	*R'z* (µm)	*S* (µm)	$S_{R'z}$ (µm)
3	10	5.510	0.089	0.028	10	6.730	0.094	0.030
4	10	6.250	0.139	0.044	10	5.750	0.086	0.027
5	10	5.740	0.116	0.037	10	4.890	0.084	0.026
6	10	5.410	0.106	0.033	10	4.870	0.085	0.027
7	10	5.210	0.088	0.028	10	4.870	0.067	0.021
7.5	10	5.440	0.102	0.032	10	4.230	0.076	0.024
8	10	6.060	0.122	0.039	10	4.340	0.095	0.030
9	10	5.970	0.096	0.030	10	5.320	0.0118	0.037
10	10	4.460	0.106	0.034	10	5.240	0.070	0.022
11	10	5.510	0.099	0.031	10	4.790	0.090	0.028
12	10	5.450	0.098	0.032	10	4.140	0.079	0.025

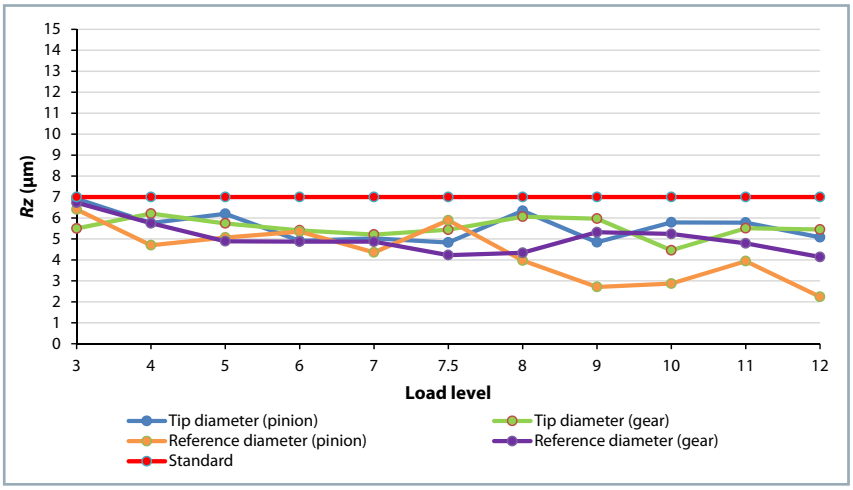

Fig. 4 Dependence of change in the maximum height of the assessed profile *Rz* on load level for TiAlN+DLC in OMW Biogear S150

lubricated with conventional oil OMW Biogear S150. There are 5 lines in the graph showing the reference and tip diameters for the pinion and the gear and limit value of the maximum height of the assessed profile *Rz* defined by the standard. These lines are colour-coded for better clarity. Tables 9 and 10 show that the maximum value of the assessed profile *Rz* did not reach a limit value of 7 µm.

Fig. 5 shows a change in the maximum height of the assessed profile *Rz* depending on load level for both the pinion and the gear. Gear pair was coated by PVD coating TiAlN + DLC and lubricated with conventional oil MADIT PP 90H. There are 5 lines in the

Table 11 Values of the maximum height of the assessed profile *Rz* (pinion, TiAlN + DLC, MADIT PP 90H)

Load level	Tip diameter				Reference diameter			
	n	*R'z* (µm)	*S* (µm)	$S_{R'z}$ (µm)	*n*	*R'z* (µm)	*S* (µm)	$S_{R'z}$ (µm)
3	10	4.770	0.072	0.023	10	3.680	0.081	0.026
4	10	5.260	0.061	0.019	10	3.270	0.058	0.018
5	10	4.830	0.071	0.023	10	3.410	0.082	0.026
6	10	5.770	0.073	0.023	10	3.420	0.063	0.020
7	10	5.570	0.069	0.022	10	3.590	0.062	0.019
7.5	10	5.480	0.077	0.024	10	2.960	0.085	0.027
8	10	3.540	0.059	0.019	10	2.550	0.098	0.031
9	10	5.010	0.063	0.020	10	3.110	0.083	0.026
10	10	5.260	0.090	0.029	10	3.630	0.087	0.028
11	10	4.990	0.069	0.022	10	3.890	0.110	0.035
12	10	4.310	0.064	0.020	10	4.470	0.085	0.027

Table 12 Values of the maximum height of the assessed profile *Rz* (gear, TiAlN+DLC, MADIT PP 90H)

Load level	Tip diameter				Reference diameter			
	n	*R'z* (µm)	*S* (µm)	$S_{R'z}$ (µm)	*n*	*R'z* (µm)	*S* (µm)	$S_{R'z}$ (µm)
3	10	5.530	0.086	0.027	10	5.680	0.078	0.025
4	10	6.560	0.089	0.028	10	5.210	0.074	0.023
5	10	4.750	0.105	0.033	10	5.910	0.091	0.029
6	10	3.810	0.090	0.028	10	4.360	0.086	0.027
7	10	5.870	0.074	0.024	10	6.050	0.096	0.030
7.5	10	6.440	0.104	0.033	10	3.410	0.077	0.024
8	10	4.780	0.107	0.034	10	5.470	0.091	0.029
9	10	5.720	0.0106	0.033	10	4.580	0.088	0.028
10	10	6.610	0.117	0.037	10	2.930	0.087	0.027
11	10	4.480	0.085	0.027	10	3.290	0.112	0.036
12	10	5.640	0.117	0.037	10	2.990	0.104	0.033

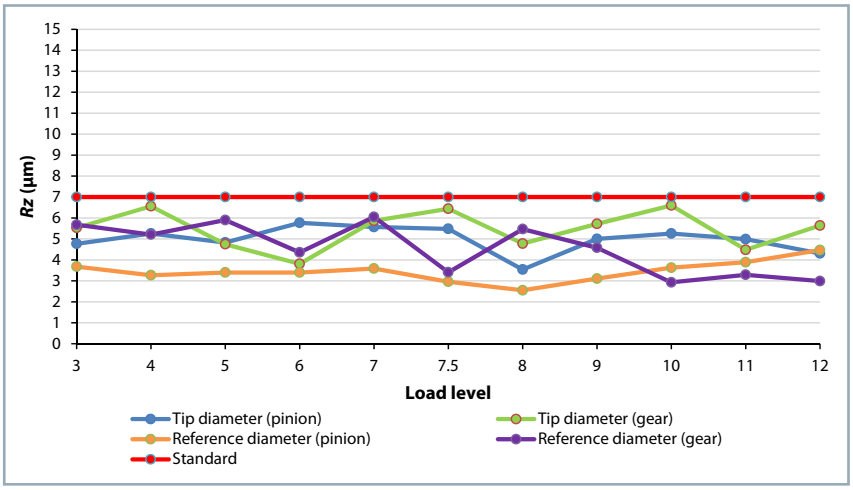

Fig. 5 Dependence of change in the maximum height of the assessed profile *Rz* on load level for TiAlN+DLC in MADIT PP 90H

graph showing the reference and tip diameters for the pinion and the gear and limit value of the maximum height of the assessed profile *Rz* defined by the standard. These lines are colour-coded for better clarity. Tables 11 and 12 show that the maximum value of the assessed profile *Rz* did not reach a limit value of 7 µm.

In comparison to research previously carried out at the Centre of Innovations of the Slovak University of Technology in Bratislava, it is possible to conclude that the adhesive properties and wear resistance of the coatings nACRo[4] and TiALN + DLC have shown better results than previously observed TiCN-MP coating + MOVIC (Mišány, 2015), since in observing those, scuffing occurred at the 11[th] load level, as well as and DLC coating (Zápotočný, 2014) where scuffing occurred at the 7[th] load level.

Conclusion

Experimental test was carried out on HCR gears coated by PVD coatings nACRo[4] and TiAlN+DLC. Conventional oil MADIT PP90H and biological oil OMW Biogear S150 were selected for lubrication environments. Both coatings were deposited in ACR PVD mode with the π411PLUS device. Coatings were produced at a thickness of 7 µm and tested according to STN 65 6280 standard. Measured values were evaluated statistically in the form of tables and graphically as the dependency of the maximum height of the assessed profile *Rz* in relation to the load level. In terms of obtained values, it is evident that the maximum height of the assessed profile *Rz* did not exceed interval 7 µm established by the standard. Therefore, it can be concluded that scuffing did not occur, and adhesive properties and wear resistance of selected coatings are satisfactory for both lubricating mediums.

Acknowledgements

The contribution has been prepared within the scientific grant project VEGA 1/0227/15 „Study of tribological characteristics of the new high hard coatings on materials suitable for gearings".

References

BOBZIN, K. – BAGCIVAN, N. – GOEBBELS, N. – YILMAZ, K. – HOEHN, B. R. – MICHAELIS, K. – HOCHMANN, M. 2009. Lubricated PVD coatings for automotive applications. In Surface and Coatings Technology, vol. 204, pp. 1097–1101.

BOŠANSKÝ, M. – VEREŠ, M. – TÖKÖLY, P. – VANYA, A. 2012. Non-standard Gears. Bratislava : SUT in Bratislava, 159 pp. ISBN 9788022737135. (In Slovak: Neštandardné ozubené prevody).

BOŠANSKÝ, M. – VANYA, A. – ČAPLOVIČ, Ľ. – HUDÁKOVÁ, M. – SONDOR, J. 2013a. Evaluation of properties of selected coatings on Aisi Grade 18Ni(250) maraging steel in terms of their use in gears. In Advanced Materials Research, vol. 746, pp. 179–185.

BOŠANSKÝ, M. – VANYA, A. – VEREŠ, M. 2013b. Evaluation of properties of selected coatings on steel C60E in terms of their use in gearing. In Advanced Materials Research, no. 25, pp. 81–85.

BOŠANSKÝ, M. – RUSNÁK, J. 2017. Assessment of options for applications TICN-MP + movic deposited on the convex-concave gearing working in interaction with the ecological lubricant. In Proceedings of 58th International Conference of Machine Design Departments. ICMD 2017. Prague : Czech University of Life Sciences Prague, pp. 44–49.

BROMARK, M. – LARSSON, M. – HEDENQVIST, P. – OLSSON, M. – HOGMARK, S. 1992. Influence of substrate and surface topography on the critical surface force in scratch adhesion testing of TiN-coated steels. In Surface Coating Technology, vol. 52 pp. 195–203.

DOSTÁL, P. – ROZLIVKA, J. – KUMBÁR, V. 2019. Operational degradation of engine oil in agricultural technology. In Acta Technologica Agriculturae, vol. 22, no. 1, pp. 17–21.

HATAMLEH, O. – SMITH, J. – COHEN, D. – BRADLEY, R. 2009. Surface roughness and friction coefficient in peened friction stir welded 2195 aluminum alloy. In Applied Surface Science, vol. 255, no. 16, pp. 7414–7426

HOEHN, B. R. – OSTER, P. – TOBIE, T. – MICHAELIS, K. 2008. Test methods for gear lubricants. In Goriva i Maziva, vol. 47, no. 2, pp. 129–157.

KADNÁR, M. – RUSNÁK, J. – TKÁČ, Z. – BOŠANSKÝ, M. 2017. Tribological experiments in automobile industry. In Visnik Nacionaľnovo Techničnovo Universitetu „CHPI", no. 25, pp. 81–85.

LÜMKEMANN, A. – BEUTNER, M. – MORSTEIN, M. – KÖCHIG, M. – WENGLER, M. – CSELLE, T. – KARPUSCHEWSKI, B. 2014. A New Generation of PVD Coatings for High-Performance Gear Hobbing. In Coatings Conference. Thessaloniki, Greece, Oct.1–3, 2014.

MÁCHAL, P. – TKÁČ, Z. – KOSIBA, J. – JABLONICKÝ, J. – HUJO, Ľ. – KUČERA, M. – TULÍK, J. 2013. Design of a laboratory hydraulic device for testing of hydraulic pumps. In Acta Universitatis Agriculturae et Silviculturae Mendelianae Brunensis, vol. 61, no. 5, pp. 1313–1319.

MICHALCZEWSKI, R. – KALBARCZYK, M. – MICHALAK, M. – PIEKOSZEWSKI, W. – SZCZEREK, M. – TUSZYNSKI, W. – WILCZYNSKI, J. 2013. New scuffing test methods for the determination of the scufing resistance of coated gears. In Tribology – Fundamentals and Advancements, vol. 12, no. 4, pp.187–215.

MIŠÁNY, J. 2015. Influence of the building machine transmission and the possibility to increase its carrying capacity with a focus to reduce the environmental load of soil. Bratislava : SUT in Bratislava, 115 pp. (In Slovak: Vplyv prevodového ústrojenstva stavebného stroja a možnosti zvýšenia jeho únosnosti so zameraním na zníženie ekologického zaťaženia pôdy).

PENGBO, M. I. – JINING, H. E. – YANFANG, Q. – KAI, C. 2017. Nanostructure reactive plasma sprayed TiCN coating. In Surface and Coatings Technology, vol. 309, pp. 1–5

RACKOV, M. – MILOVANČEVIĆ, M. – KANOVIĆ, Ž. – VEREŠ, M. – RAFA, K. – BANIĆ, M. – MILTENOVIĆ, A. 2014. Optimalization of HCR gearing geometry using generalized particle swarm optimalization algorithm. In Modern Methods of Construction Design, vol. 109, no. 10, pp. 539–545.

STN 656280: 1985 Lubricants. Mechanical testing of lubricants in the FZG gear ring test machine.

TULÍK, J. – HUJO, Ľ. – KOSIBA, J. – JABLONICKÝ J. – JÁNOŠOVÁ, M. 2017. Evaluation of new biodegradable fluid on the basis of accelerated durability test, FTIR and ICP spectroscopy. In Research in Agricultural Engineering, vol. 63, no. 1, pp. 1–9.

TULÍK, J. – KOSIBA, J. – BUREŠ, Ľ. – ŠINSKÝ V. 2013. Analysis of synthetic oil samples during an operating test. In Acta Technologica Agriculturae, vol. 16, no. 1, pp. 21–24

ZÁPOTOČNÝ, J. 2014. Analysis of qualitative and quantitative characteristics of placed films in the system 'film – cog side' from the tribological point of view. Bratislava : SUT in Bratislava. (In Slovak: Určenie kvalitatívnych a kvantitatívnych charakteristík deponovaných povlakov v systéme povlak bok zuba z tribologického hľadiska).

sciendo

DOI: 10.2478/ata-2019-0010

Acta Technologica Agriculturae 2
Nitra, Slovaca Universitas Agriculturae Nitriae, 2019, pp. 56–59

TITANIUM AND STAINLESS STEEL MIG LSC WELDING

Nela POLÁKOVÁ*, Petr DOSTÁL

Mendel University in Brno, Czech Republic

This paper deals with the issue of welding two different materials – titanium and stainless steel (UNS N50400 + X5CrNi 18-10). These two materials have completely different chemical compositions and mechanical properties; therefore, process of their mutual welding is complicated. Melting temperature of both materials is also different. An innovative MIG LSC arc welding method with an additional material has been selected for this purpose. A protective atmosphere was used in order to avoid galvanic corrosion of materials that would preclude the welding process. Aforementioned atmosphere contained 100% Ar. The MIG LSC welding method was designed by Fronius. Presented experiment compares utilization of following 4 different electrodes (additional material) for the welding of titanium and stainless steel: Ti, Fe, corrosion-resistant Fe and CuSi3 electrode. Tensile test was utilized for evaluation of weldment mechanical properties. Measured results were supplemented with a metallographic analysis snapshot and tensile diagram.

Keywords: welding; titanium; stainless steel; MIG LSC; CuSi3 welding electrode

Multiple industries, such as nuclear industry, are interested in welding of two different corrosion-resistant materials: stainless steel and titanium. Titanium and stainless steel cannot be welded reliably, because these materials are characteristic by mutual metallurgical incompatibility. This is due to the formation of brittle intermetallic compounds that arise when titanium is welded with stainless steel (Pardal et al., 2016). Ability to create a heterogeneous weld of different metals is determined by their weldability. Fusion welding involves mixing of basic materials (possibly with additional material). Problems associated with fusion welding of titanium were observed by e.g. Sagar et al. (2018). Weldability is a term that indicates the ability of a particular material (metal) to form a weld. Weld is used to join the material (Hluchý and Kolouch, 2002). Weld can be made using a combination of high temperature required to melt the material and necessary pressure. Issue of weldment quality created by arc welding was observed by Hluchý et al. (2002). Welding process includes three phases: melting phase, solidification phase and cooling phase, which it easiest to carry out. If materials characteristic with guaranteed weldability or reduced weldability (this information is given by the material manufacturer) are welded, it is advisable to weld them by means of an electrode welding process with an additional electrode (Černý et al., 2016a). Variety of corrosion complications tends to occur during welding. However, with the development of new technologies, operational parameters, and new aggressive substances, these combinations become increasingly complex. Problems caused by corrosion of metals and welds adversely affect industrial development. They cause considerable damage, so it is important to pay attention to corrosion and eliminate it as much as possible (Šustr et al., 2016). For the aforementioned reasons, it is advisable to use corrosion-resistant metal materials. However, corrosion affects not only metals, but also non-metallic materials (corrosion of concrete, glass and plastics). Material protection against corrosion can be ensured in numerous different ways. The most common method for protection of materials against corrosion, especially metal, includes the usage of a protective surface (e.g. paint), correcting the corrosive environment (a complex solution in some cases). The most reliable protection lies in selection of a suitable material (Talbot and Talbot, 2019). Considering the welding of corrosion-resistant materials, it is also necessary to select a suitable protective atmosphere.

Material and methods

Purpose of the experiment was to find out a suitable additional material in order to create a heterogeneous weldment using the MIG LSC method. Two basic materials (difficult to weld together) were welded – UNS N50400 titanium and X5CrNi 18-10 stainless steel. These basic materials were selected because of their complex welding process and need for joining these two materials for the purposes of nuclear and chemical industries. All in all, 4 different electrodes in total were gradually used for welding. Each electrode was used for welding of 10 samples. Consequently, 40 samples were welded and subsequently analysed. Table 1 shows two basic materials and their chemical composition.

Contact address: Nela Poláková, Mendel University in Brno, Faculty of AgriSciences, Department of Technology and Automobile Transport, Zemědělská 1, 613 00 Brno, Czech Republic, e-mail: nela.polakova@mendelu.cz

Table 1 Basic materials

Basic material 1	Titanium Grade 2 (UNS N50400)	Ti 99.375%; Fe max. 0.25%; O max. 0.25%; C max. 0.08%; N max. 0.03%; H max. 0.015%; Density 4.51 g·cm^3
Basic material 2	Austenitic chromium-nickel steel (X5CrNi18-10)	Fe 68.805%; Cr 18%; Ni 10%; C 0.12%; Mn 2%; Si 1%; P 0.045%; S 0.03%

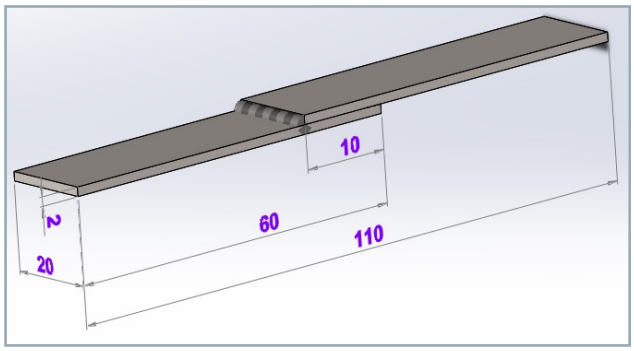

Fig. 1 Dimensions of welded samples

Titanium Grade 2 (UNS N50400) supplied by the Bibus metals s.r.o. company was used to create a heterogeneous weldment using the MIG LSC method. It is the most widely commercially used clean titanium, providing an excellent balance of strength and ductility. This material is tough and easily weldable. The second basic material for the welding was austenitic chromium-nickel unstabilized steel labelled as X5CrNi18-10 (according to the ČSN EN 10088-1:2015, EN 1.4301 standard) delivered by the JM20 s.r.o. company. Dimensions (mm) of these materials can be seen in Fig. 1.

Traditional welding method of MIG to weld manganese steel was attempted by Bernát et al. (2013), but weld quality was not optimal. Therefore, innovative welding method MIG LSC was selected for the purposes of this experiment, which was designed by Fronius in order to increase the quality of welded joints. Four welding electrodes were used for MIG LSC welding.

Types of welding electrodes:

1. Titanium electrode (AWS A 5.16 ERTi-1): chemical composition – 99.375% Ti, 0.25% Fe, 0.25% O, 0.08% C, 0.03% N, 0.015% H.
2. Stainless electrode (1.4316): chemical composition – 69.22% Fe, 19% Cr, 10% Ni, 1.7% Mn, 0.08% C.
3. Fe electrode (1.5130): chemical composition – 97.32% Fe, 1.65% Mn, 0.95% Si, 0.08% C.

Table 2 Parameters of welding equipment Fronius TPS 400i

Electrode feed speed	9.0 m·min^{-1}
Welding current	104 A
Welding voltage	17.5 V
Arc length correction	0.0
Pulse/dynamics correction	-1.0
Arc length stabilisation	0.5
Frequency	3.0 Hz
Gas flow	15.0 l·min^{-1}

4. CuSi3 electrode (S Cu 6560): chemical composition – 97% Cu and 3% Si.

In all cases, protective atmosphere of the welding bath contained 100% argon due to a high gas absorption rate of titanium at temperatures exceeding 600 °C.

The MIG LSC – low spatter control welding method was used to melt the additional material in the form of an electrode with the diameter of 1 mm. This is an arc control method for minimum spraying. From a technological point of view, it is soldering by means of an electrical arc as a heat source in order to melt the additional material. For this reason, term welding was utilized in the paper. Table 2 shows welding parameters of equipment Fronius TPS 400i (supplier Austria – Wels) – values given come from the welding device records.

Results and discussion

Cracks occurred in welds due to the formation of brittle intermetallic compounds between FeTi and Fe2Ti when using both titanium and corrosion-resistant electrodes (Figs. 2a, 2b). Other adverse effects included great difference of the thermal expansion coefficient in the additional material and basic materials. Fig. 2 shows cracks in welds between the additional material (stainless electrode; titanium electrode) and one of the basic materials (titanium).

When a Fe electrode was used, the weld broke off completely after a few seconds and material was broken down due to an extreme internal stress caused by the large differences in cooling and subsequent shrinking of different metals (Fig. 2c). These metals have different thermal expansion coefficient. The only electrode, by means of which a permanent heterogeneous joint was achieved, was CuSi3 electrode. Considering the samples in which a crack occurred in the weld (Fig. 2a, 2b, 2c), they have not been submitted to tensile tests, since these were not welded. Samples that were successfully welded were submitted to tensile test in order to observe their mechanical properties. All 10 successfully welded samples showed almost identical course of tensile diagram. The best results achieved in the tensile test using CuSi3 electrode are shown on an example of selected sample in Fig 3.

Representative sample was selected for the best properties. At point B, Fig. 3 shows the maximum stress needed to break the weldment, which amounted to 98 MPa.

Tensile strength of basic non-welded titanium material is 345 MPa and tensile strength of the basic non-welded stainless steel material is 520 MPa. These values are given to compare the mechanical properties of non-welded base materials. Decrease in weld tensile strength was caused by welding, which adversely affected the material mechanical properties. Further negative effects of welding included the heterogeneity of the joint materials. Despite this, the

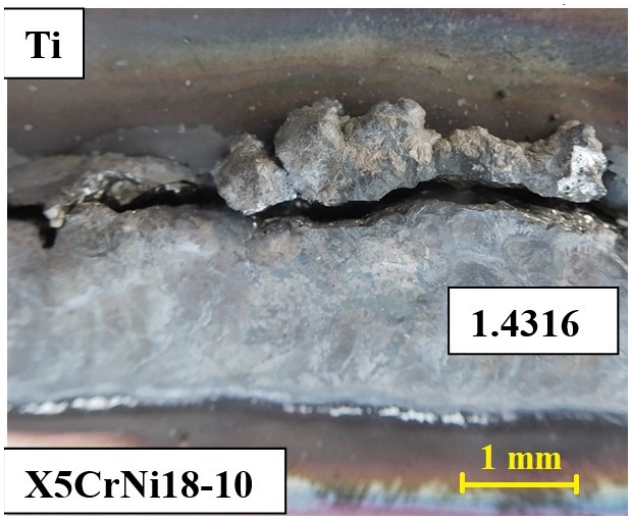

2a

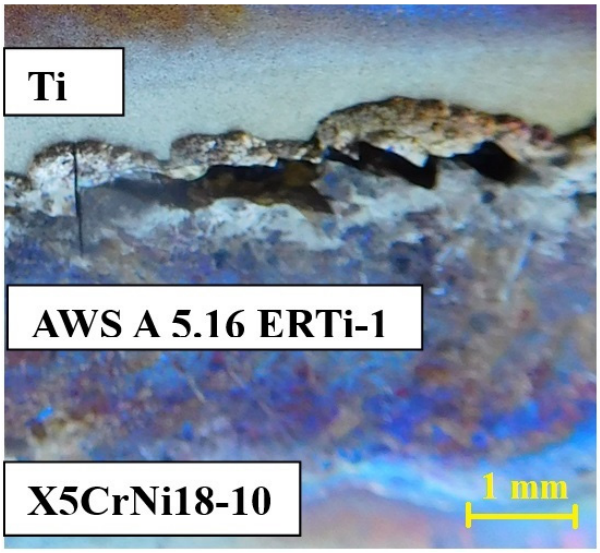

2b

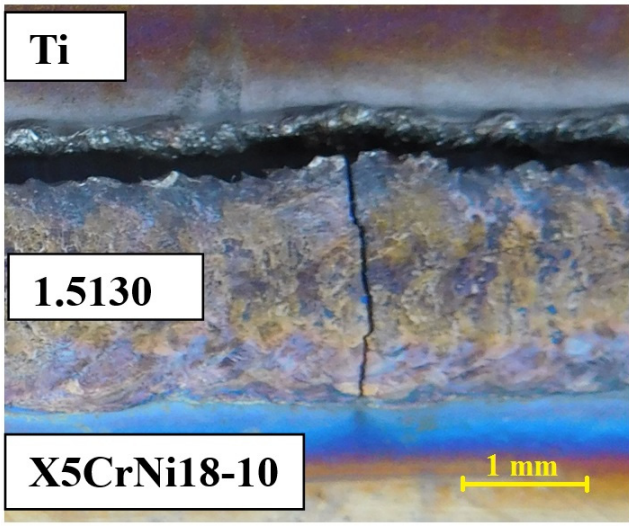

2c

Fig. 2 Cracks in welds: 2a – stainless electrode 1.4316; 2b – titanium electrode (AWS A 5.16 ERTi-1); 2c – Fe electrode

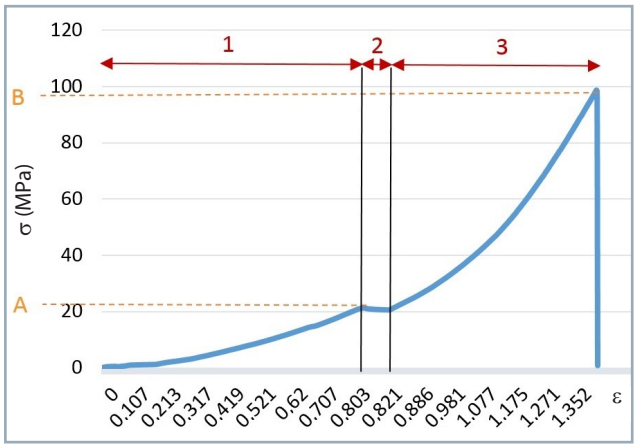

Fig. 3 Tensile test results: A (stress on yield strength) = 21 MPa; B (stress on strength) = 98 MPa
1 – flexible deformation area; 2 – yield strength; 3 – plastic deformation area

welding was successful. Relative elongation of epsilon of the welded joint at the break amounted to 1.35, which represents 135% of original length of welded joint. Point A shows yield stress amounting to 21 MPa. In terms of area 1, only flexible deformation occurs; area 2 shows yield stress and area 3 shows plastic deformation. Fracture was observed in static tensile test of the weld joint. Samples were further observed through metallographic analysis conducted by Honeywell. Microstructure etching was produced using nitric acid. Welding zone microstructure in Fig. 4 consists of a metal (stainless steel X5CrNi10-10), diffusion layer of 0.4 mm and additional material (CuSi3) consisting of copper and copper silicate. Copper atoms penetrate the steel along the grain boundaries, creating a connection in the area of surface layers.

In regards to the high rate of titanium gas absorption (N, O, H) at temperatures exceeding 600 °C, all methods not using a special argon protection, vacuum soldering or a special flux can be excluded for titanium soldering. Titanium reacts very well with melted metals, producing solid solutions with aluminium and carbon. Elements such as Cu, Cr, Fe, Mn, Ag, Co, Si and Sn have a limited solubility in both α and β phases of titanium. In fusion with titanium, they form an equilibrium diagram with the eutectoid.

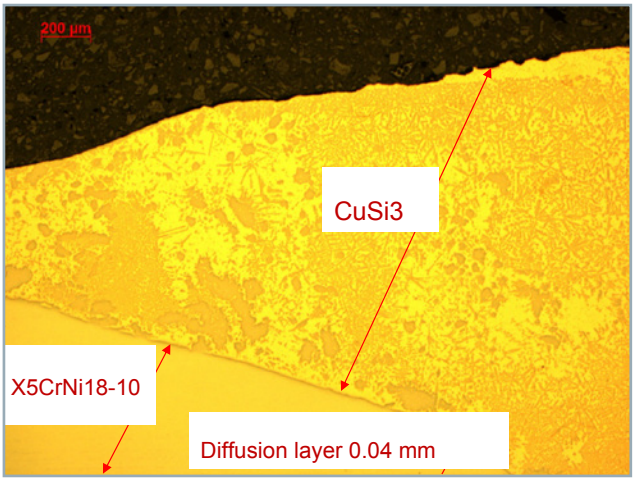

Fig. 4 Welding zone microstructuredeformation area

Therefore, at an equilibrium state, β phase falls into a solid solution and γ phase becomes enriched by an alloy. As the content of mentioned elements increases, temperature of the recrystallization also increases, resulting in expansion of γ phase stability. The maximum Cu solubility (1.5%) in Ti is achieved at temperature of 798 °C. At temperature range of 400–600 °C, only 0.4–0.6% of Cu is dissolved in Ti. At temperatures below 300 °C, this solubility changes only a little. Eutectoid arises at the Cu content of 7%. Since Cu forms a number of intermediary phases with Ti, it is not a suitable material for soldering. The Cu content in silver solders should be as low as possible, so that soldering at temperatures below 98 °C might be possible (Mousavi and Sartangi, 2008). If the material is specified as difficult to weld by the manufacturer, it is recommendable to use a CuSi3 electrode. It is possible to achieve good results using this electrode, e.g. in welding of zinc-coated steel sheets with pure zinc or zinc-aluminium (Poláková et al., 2017; Matsui, 1998). Similarly to results obtained by Černý et al. (2016b), no visual external weld defects were detected and weld quality was positively evaluated. Typical tiny spheres that are always caused by molten metal splashes have been found in the immediate vicinity of the weld.

Conclusion

Due to its high strength to weight ratio, titanium and its alloys are suitable for use in modern industry. Another valued property of titanium is its corrosion resistance (Boyer, 1996). Commercially pure titanium was successfully processed during the exhaust pipe and muffler manufacturing process. This material is used for its good mechanical properties, chemical resistance and for its high quality (and desired) surface appearance.

High wear resistance of titanium and its alloys can be useful e.g. in engine intake valves. Titanium is also resistant to cyclic stress and high temperatures (due to its high melting point). These advantages can be useful e.g. in engines with higher power, not only motorcycles (Fujii et al., 2003). Many industries use a combination of corrosion-resistant steel with titanium. Creating heterogeneous joints in materials with different physical and mechanical properties is always problematic (Moravec et al., 2017). In experiment presented, CuSi3 electrode showed the best results, since it was the only electrode type, by means of which a permanent joint was achieved. Utilization of other electrodes was completely unsuccessful. Therefore, hypothesis presented by Chen et al. (2014) in terms of how difficult it is to weld titanium alloys with steel due to large differences in thermal, physical and chemical properties has been confirmed. Results obtained are in line with Pardal et al. (2016), confirming that it is possible to join a stainless steel and Ti by means of CuSi3 welding electrode utilizing a protective atmosphere of clear argon. The maximum tensile strength achieved by means of MIG LSC welding was 98 MPa. Experiment results showed that hypothesis presented by Mousavi and Sartangi (2008) – that Cu is not suitable as material for soldering of titanium joints – has not been confirmed.

Acknowledgement

The research has been supported by the project TAČR GAMA TG02010074 (part 201801) – PARKISS.

References

BERNÁT, R. – ZÁLEŽÁK, Z. – KECSKÉS, N. – BLAŠKO, P. 2013. Assessing the weld quality of manganese steel. In Acta Technologica Agriculturae, vol. 16, no. 4, pp. 99–102.

BOYER, R. R. 1996. An overview on the use of titanium in the aerospace industry. In Materials Science and Engineering, vol. 213, no. 1–2, pp. 103–114.

ČERNÝ, M. – DOSTÁL, P. – MAZAL, P. – ŠUSTR, M. 2016a. Verification of the quality of the weld when utilising the MAG/CO 2 method. In Acta Universitatis Agriculturae et Silviculturae Mendelianae Brunensis, vol. 64, no. 1, pp. 31–42.

ČERNÝ, M. – DOSTÁL, P. – ŠUSTR, M. 2016b. Visualization of the coated electrode welding. In Acta Universitatis Agriculturae et Silviculturae Mendelianae Brunensis, vol. 64, no. 1, pp. 43–51.

ČSN EN 10088-1: 2015. Stainless Steel – Part 1: Stainless Steel Overview. Praha: Český normalizační institut. (In Czech: Korozivzdorné oceli – Část 1: Přehled korozivzdorných ocelí).

FUJII, H. – TAKAHASHI, K. – YAMASHITA, Y. 2003. Application of titanium and its alloys for automobile parts. In Nippon steel technical report, Shinnittetsu giho, vol. 378, no. 88, pp. 62–67.

HLUCHÝ, M. – KOLOUCH, J. 2002. Engineering Technology 1 – Part 1: Materials Science. 1st ed., Praha : Scientia, spol. s r. o. 266 pp. ISBN 8071832626. (In Czech: Strojírenská technologie 1 – 1. díl Nauka o materiálu).

HLUCHÝ, M. – MODRÁČEK, O. – PAŇÁK, R. 2002. Engineering Technology 1 – Part 2: Metallography and Heat Treatment. Praha : Scientia, spol. s r. o., 173 pp. ISBN 8071832650. (In Czech Strojírenská technologie 1 – 2. Díl: Metalografie a tepelné zpracování).

CHEN, S. – ZHANG, M. – HUANG, J. – CUI, C. – ZHANG, H. – ZHAO, X. 2014. Microstructures and mechanical property of laser butt welding of titanium alloy to stainless steel. In Materials & Design, vol. 53, pp. 504–511.

MATSUI, H. 1998. Arc welding technologies of galvanized steel sheet for automotive underbody. In Proceedings of 4th International Conference on Zinc and Zinc Alloy Coated Steel Sheet. Japan : The Iron and Steel Institute, pp. 778–784.

MORAVEC, J. – DIKOVITS, M. – BEAL, M. C. – NOVAKOVA, I. – CHANDEZON, R. – SOBOTKA, J. 2017. Selection of the proper diffusion welding parameters for the heterogeneous joint Ti grade 2/AISI 316L. In Manufacturing Technology, vol. 2, pp. 231–237.

MOUSAVI, S. A. – SARTANGI, P. F. 2008. Effect of post-weld heat treatment on the interface microstructure of explosively welded titanium–stainless steel composite. In Materials Science and Engineering: vol. 494, no. 1–2, pp. 329–336.

PARDAL, G. – GANGULY, S. – WILLIAMS, S. – VAJA, J. 2016. Dissimilar metal joining of stainless steel and titanium using copper as transition metal. In The International Journal of Advanced Manufacturing Technology, vol. 86, no. 5–8, pp. 1139–1150.

POLÁKOVÁ, N. – DOSTÁL, P. – ČERNÝ, M. – VOTAVA, J. – DOBROCKY, D. 2017. Effect of heat treatment of CMT weld on its mechanical properties. In: MendelNet Proceedings of International PhD Students Conference. Mendel University in Brno, pp. 802–807. ISBN 9788075095299.

SAGAR, D. B. A. – VIKAS, B. – SAHA, B. – NARASIAH, N. – JAYAPAL, P. – RAM, G. D. J. – RAO, M. S. K. 2018. Study of microstructure and mechanical properties of friction welded metastable beta titanium alloy titan 1023. In Materials Today Proceedings, vol. 5, no. 9, pp. 20760–20768.

ŠUSTR, M. – DOSTÁL, P. – ZAČAL, J. 2016. The acoustic emission for monitoring the hardness of the cold metal transfer weld. In Acta Universitatis Agriculturae et Silviculturae Mendelianae Brunensis, vol. 64, no. 2, pp. 543–547.

TALBOT, D. E. J. – TALBOT, J. D. R. 2019. Corrosion Science and Technology. 2nd ed., Florida : CRC Press LLC. 432 pp. ISBN 1420049887.

sciendo

DOI: 10.2478/ata-2019-0011

Acta Technologica Agriculturae 2
Nitra, Slovaca Universitas Agriculturae Nitriae, 2019, pp. 60–63

THE HEADER FOR A BREEDING PLOT COMBINE FOR SUNFLOWER HARVESTING

Vasiliy Dmitrievich SHAFOROSTOV, Sergey Sergeevich MAKAROV*

V.S. Pustovoit All-Russian Research Institute of Oil Crops, Krasnodar, Russian Federation

Usage of modern technical means for sunflower harvesting, due to their construction designs, inevitably involves yield losses reaching up to 10–11%, as well as increasing of seed injury. Aim of the research presented was to develop a header for a breeding plot combine for sunflower harvesting. As a result, an experimental four-row header for the Delta plot combine for sunflower harvesting was developed and manufactured. The main values of the adjustable parameters are given, depending on the biometric characteristics of the plants being harvested. Using this experimental header, seed injury did not exceed 1.51% at a moisture content of 5.1% and seed losses did not exceed 1%.

Keywords: seed harvesting; construction; four-row header; auger feeder; seed injury and seed losses

Plant height and head diameter do not depend only on the sunflower variety, but also on the cultivation zone, weather and soil conditions. Cultivated varieties and hybrids of sunflower are also characterized by a significant variation in plant height, which makes it difficult to cut and thresh exclusively the productive plant part, leading to the head loss, deterioration of the thresher and necessity to clean the combine. Due to sunflower characteristics, utilization of technical means for its harvesting is inevitably related to the crop losses and seed injury (Dalmis et al., 2013a; Dalmis et al., 2013b; Doronin, 2006; Fedorenko, 1985; Csanadi and Hamphoff, 2007; Gonulol et al., 2009; Miklič et al., 2012; Mirzabe and Chegini., 2015; Mirzabe et al., 2012; Novák and Vitázek,, 2014; Sekhon et al., 2004; Sudajan et al., 2002; Trubilin and Kravchenko, 2001).

For purposes of research, several headers for sunflower harvesting by different producers were taken into consideration; however, it was observed that companies-producer tried to improve the construction of headers, increase the reliability of equipment, yet did not change the key operating principles. Producers have still not addressed adequately the issue of how to decrease stem length attached to sunflower heads before transporting them into the threshing drum during harvest (Csanadi and Hamphoff, 2007).

In recent years, the All-Russian Research Institute of Oil Crops has been carrying out research aimed at improving the work tools for gripping, feeding and cutting of sunflower plants in order to increase the height range of the harvested plants, to provide a cut of heads with a minimum stem length, as well as to reduce the level of seed injury during threshing. Due to the inclination of feeding screws, speed of horizontal component for stem transportation through the device channels, as well as combine speed and speed of other constructive designs, the length of stems entering together with heads for threshing decreases to 0.1–0.3 m, reducing the load of threshing machine and combine cleaning system by unproductive crop (Makarov et al., 2007; Sitchenko, 2001; Čanak et al., 2011).

The research aim is to develop the header for a plot combine, which would provide a maximum cut of sunflower stem off the head regardless of its original length.

Material and methods

For that purpose, a four-row header for the Delta plot combine for harvesting breeding plots was developed and manufactured; the scheme and general overview of this equipment is shown in Figs. 1 and 2. Header design is protected by the patent of the Russian Federation no. 179951.

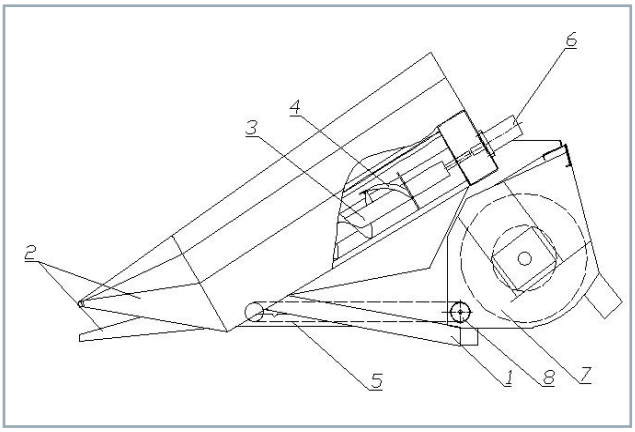

Fig. 1a Scheme of a four-row header for Delta combine for sunflower harvesting, a – side view
1 – frame; 2 – stem dividers, 3 – screws; 4 – cutting pair; 5 – belt conveyor; 6 – hydraulic motors; 7 – transverse screws of a header; 8 – drive shaft of conveyor

Contact address: Sergey Sergeevich Makarov, V.S. Pustovoit All-Russian Research Institute of Oil Crops, Krasnodar, Russian Federation, e-mail: mechanization@vniimk.ru

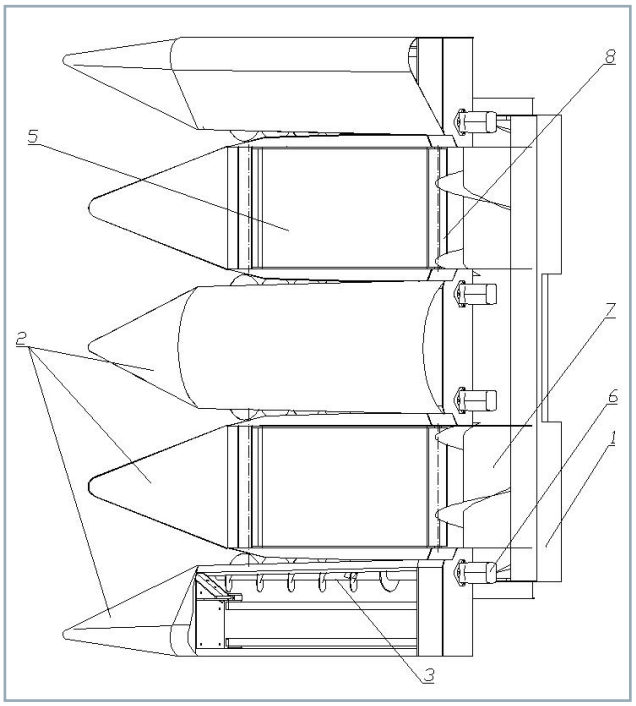

Fig. 1b Scheme of a four-row header for Delta combine for sunflower harvesting, b – top view
1 – frame; 2 – stem dividers, 3 – screws; 4 – cutting pair; 5 – belt conveyor; 6 – hydraulic motors; 7 – transverse screws of a header; 8 – drive shaft of conveyor

Fig. 2 The four-row header for Delta combine for sunflower harvesting

Fig. 3 Four-row header during harvesting of sunflower line VK-678B

Header consists of a frame [1], upon which dividers [2] with screws [3] are positioned, with a cutting pair [4] mounted on the latter. Between the dividers [2], belt conveyors [5] are horizontally placed on the frame [1]. The feeding screws [3] are driven by means of hydraulic motors [6]. A transverse feeding screw of the header [7] is installed behind the belt conveyors and the drive shaft of the belt conveyors [8] is placed under the transverse feeding auger.

The values of the main adjustable header parameters are given in Table 1.

The positive effect includes reduction of sunflower seed yield loss in harvesting of both dwarf and tall sunflower plants by a reliable technological process, as well as reduction of the length of stems attached to sunflower heads entering the combine threshing machine. The explanation is as follows. The inclination angle of the screws to the soil surface should fall within the optimal values (from 25° to 35°) depending on the biometric characteristics of sunflower plants. During sunflower harvesting, height of the lead-in part of screws should be adjusted to the minimum head height by raising and lowering the header by means of the combine hydraulic cylinder. At the same time, the inclination angle of screws [3] to the soil surface also changes and outsteps the optimal limits, resulting in an increase in the losses of whole heads. The ability to adjust the inclination angle of screws [3] to the header's plane of the frame [1] during its lowering and raising by means of the header hydraulic cylinder allows for the optimum inclination angle of screws to the soil during harvesting of both dwarf and tall sunflower plants, i.e. to reduce losses.

During harvesting of dwarf sunflower (Fig. 3), the header frame is set to the lowest position – such that the lead-in part of the stem divider is at the height equal to the minimum height of head position above the surface level; however, the cutting pair can end up higher than the plant height, which can lead to the direct losses as described above. To prevent this from happening, the operator in the combine cabin lowers the screws by means of the hydraulic cylinder, optimizing their inclination angle to the soil surface and thereby improving the technological process of harvesting and avoiding direct losses of heads and seeds.

During harvesting of tall sunflower (Fig. 4), the header frame is set to the highest position – such that the lead-in part of the stem divider is at a height equal to the minimum height of heads position above the surface level. However,

Table 1 The values of the main adjustable parameters of a header for the sunflower breeding plot combine

Properties	Line VK-678B	Variety Dzhinn
1. The grip height (m)	0.3–0.4	0.5–0.7
2. Rotation frequency of screw feeders (min^{-1})	140–150	130–140
3. Travel speed during harvesting ($km \cdot h^{-1}$)	4–5	4–5

Fig. 4 Four-row header during harvesting of sunflower variety Dzhinn

the inclination angle of the screws to the soil surface is decreasing automatically and the lower it is, the smaller the amount of stem being cut. To ensure the cutting off of the maximum amount of sunflower stem material off the head, the operator in the combine cabin lifts the frame [3] of the screws using the hydraulic cylinder, optimizing their inclination angle to the soil surface and thereby improving the technological process of harvesting – reducing the cut length of stems and headers entering the threshing machine, thereby preventing the indirect losses of certified sunflower seeds. Screws adjusted to an optimal angle to soil surface during the combine traveling guarantee decreasing the cut stem length cutting, as well as head and seed losses.

Minimal losses in whole heads and free seeds, as well as the increased cut length of stem attached to the head that enter the threshing machine can be attributed to the header operation quality indicators during sunflower harvesting.

The inclination angle of the screws to the field surface was set in three positions: 25°, 35°, 45°.

The losses of entire heads and free seeds were determined according to the Russian National Standard 28301-2015 (GOST 28301–2015). Twine frames were laid to record losses at each record passage (not less than 100 meters). To determine losses of whole heads, the frame area was limited to 1.4 m widthwise and 3 m lengthwise. To determine losses of free seeds, the frame area was limited to 1.4 m widthwise and 0.15 m lengthwise. Three frames were laid on each record passage. The obtained data was recorded in the register of input data.

The obtained experimental data was processed by methods of mathematical statistics. A total of 14 ha of seed production plots of sunflower varieties and about three thousand breeding plots were harvested.

The cut length of stems on the head was determined indirectly. The cut length of the stems remaining in the field on root was measured after the passage of the combine equipped with the experimental header. The obtained data was statistically processed and compared with the biometric characteristics of plants prior to harvesting.

Results and discussion

Experimental research was carried out in accordance with the Russian National Standard 28301-2015 (GOST 28301–2015).

The main performance properties of the Delta breeding plot combine with a four-row header are provided in Table 2 and 3.

The analysis of the obtained data shows that the size of stem cut with head is almost the same in dwarf hybrid plants and in Dzhinn plants – a tall confectionery variety – at 15.0 and 25.8 cm, respectively. The fact that the heads enter the thresher of the combine only with such small stem material amounts significantly improves the combine performance.

Confectionery Dzhinn variety was chosen to study the obtained bulk, since its seed coat is less resistant to the impact of applied force.

Characteristics of the obtained seed bulk of sunflower variety Dzhinn were determined according to the Russian

Table 2 The main performance properties of the Delta breeding plot combine with a four-row header during harvesting of sunflower hybrid VK 678 B

Properties	Arithmetic average (cm)	Standard deviation (cm)	Error of sampling average (cm)	Variation factor (%)	Relative error of sampling average (%)
Length of a stem before cutting of heads (cm)	146.9	6.5	0.7	4.41	0.46
Length of a stem after cutting of heads (cm)	131.9	13.7	1.4	10.38	1.01
Losses (%)	0.25				

Table 3 The main performance properties of Delta breeding plot combine with four-row header during harvesting of sunflower variety Dzhinn

Properties	Arithmetic average (cm)	Standard deviation (cm)	Error of sampling average (cm)	Variation factor (%)	Relative error of sampling average (%)
Length of a stem before cutting of heads (cm)	199.1	17.68	1.86	8.88	0.94
Length of a stem after cutting of heads (cm)	173.2	20.5	2.16	11.84	1.2
Losses (%)	0.97				

Table 4 Characteristics of seeds of Dzhinn sunflower variety harvested by the Delta breeding plot combine with a four-row header

No.	Characteristics	Mean value of characteristics (%)
1.	Seed content of the main crop	
	– total	96.64
	– including hulled	1.11
2.	Waste products	
	– broken sunflower seeds	0.40
	– shrunk, unformed seeds	1.58
	– organic impurity	1.38

National Standard 12037-81 (GOST 12037-81) and are provided in Table 4.

The analysis of the presented data shows that the purity of the bulk taken in by a combine equipped with the new header is 96.64%; seed injury is only 1.51% at a moisture content of 5.1%, which indicates that the threshing device works well, and seed losses do not exceed 1%.

Conclusion

The research results show that the Delta breeding plot combine equipped with a new four-row header enables harvesting of both dwarf and tall sunflower plants with the least possible losses. The header working tools provides a maximum cut-off of sunflower stems from the heads, regardless of their initial length. Since sunflower heads enter the threshing drum only with small stem material, optimal conditions are created for complete threshing of seeds, while the purity of the received bulk is much higher than purity provided by other equipment.

References

ČANAK, P. – JOCKOVIČ, M. – CIRIC, M. – MIROSAVLJEVIČ, M. – MIKLIČ, V. 2011. Effect of chemical desiccation application moment on germination energy of sunflower seed. In Selekcija i Semenarstvo, vol. 17, no. 2, pp. 41–47.

CSANADI, T. – HAMPHOFF, B. 2007. A header for efficient sunflower harvesting Deployment of special sunflower head. In Engineering Solutions for Energy and Food production 2007'. VDI Berichte, vol. 2007, pp. 343–346. ISBN 9783180920016.

DALMIS, I. S. – KAYISOGLU, B. – BAYHAN, Y. – ULGER, P. – TORUK, F. – DURGUT, F. 2013a. Development of a chopper unit for chopping of sunflower stalk during harvesting by combine harvester. In Bulgarian Journal of Agricultural Science, vol. 19, no. 5, pp. 1148–1154.

DALMIS, I. S. – KAYISOGLU, B. – BAYHAN, Y. – TORUK, F. – DURGUT, F. T. 2013b. Determination of the effects of rotation speed and forward speed on combine harvester driven stalk chopper assembly operating performance. In Tarim Bilimleri Dergisi, vol. 19, no. 1, pp. 54–62.

DORONIN, E. F. 2006. The optimum work modes of a header during sunflower harvesting. In Tractors and Agricultural Machines, no. 2, pp. 9–10.

FEDORENKO, E. G. 1985. Decrease of seed injury during harvesting. In Equipment in Agriculture, no. 8, p. 59.

GONULOL, E. – DALMIS, I. S. – KAYISOGLU, B. – BAYHAN, Y. – KOCABIYIK, H. 2009. The evaluation of alternative stalk chopping methods in sunflower farming. In African Journal of Agricultural Research, vol. 4, no. 12, pp. 1398–1403.

GOST 12037-81. Seed of farm crops. Methods for determination of purity and seed lot impurity.

GOST 28301–2015. Grain harvesters. Test methods.

MAKAROV, S. S. – SHAFOROSTOV, V. D. – SUKHOMLINOV, L. G. – MIKHAILOVA, V. L. 2007. Determination of optimal conditions of sunflower harvesting by a combine with a transverse rotor. In Oil Crops: Scientific and technical bulletin of All-Russian Research Institute of Oil Crops, vol. 137, no. 2, pp. 119–123.

MIKLIČ, V. – MRDJA, J. – MODI, R. – JOCIČ, S. – DUŠANIČ, N. – HLADNI, N. – MILADINOVIČ, D. 2012. Effect of location and harvesting date on yield and 1,000-seed weight of different sunflower genotypes. In Romanian Agricultural Research, no. 29, pp. 219–225.

MIRZABE, A. H. – CHEGINI, G. R. 2015. Measuring picking force of sunflower seeds and prediction of reasonable range of air-jet parameters to remove sunflower seeds from the head. In Agricultural Engineering International: CIGR Journal, vol. 17, no. 3, pp. 415–429.

MIRZABE, A. H. – KHAZAEI, J. – CHEGINI, G. R. 2012. Physical properties and modeling for sunflower seeds. In Agricultural Engineering International: CIGR Journal, vol. 14, no. 3, pp. 190–202.

NOVÁK, J. – VITÁZEK, I. 2014. Electrical properties of sunflower achenes. In Acta Technologica Agriculturae, vol. 17, no. 4, pp. 109–113.

SEKHON, N. K. – HIRA, G. S. – SIDHU, A. S. – THIND, S. S. 2004. Determination of optimum time for harvesting of sunflower (Helianthus annuus). In Indian Journal of Agricultural Sciences, vol. 74, no. 7, pp. 394–395.

SITCHENKO, E. I. 2001. About reducing losses of sunflower seeds during mechanized harvesting. In Oil Crops: Scientific and technical bulletin of All-Russian Research Institute of Oil Crops, no. 124, pp. 183–185.

SUDAJAN, S. – SALOKHE, V. M. – TRIRATANASIRICHAI, K. 2002. Effect of type of drum, drum speed and feed rate on sunflower threshing. In Biosystems Engineering, vol. 83, no. 4, pp. 413–421.

TRUBILIN, E. I. – KRAVCHENKO, V. S. 2001. Justification of possibility of sunflower harvesting by grain headers of combines. In Equipment in Agriculture, no. 1, pp. 20–22.

sciendo

DOI: 10.2478/ata-2019-0012

Acta Technologica Agriculturae 2
Nitra, Slovaca Universitas Agriculturae Nitriae, 2019, pp. 64–69

DETERMINATION OF TOXIC METALS CONTENT IN IRANIAN AND ITALIAN FLAVOURED OLIVE OIL

Parisa ZIARATI[1]*, Fatemehsadat MIRMOHAMMAD MAKKI[2], Sergij VAMBOL[3], Viola VAMBOL[3]

[1]Nutrition and Food Sciences Research Center, Tehran Medical Sciences, Islamic Azad University, Tehran, Iran;
[2]Islamic Azad University, Tehran, Iran
[3]Berdyansk State Pedagogical University, Berdyansk, Ukraine

Cultural practices and control of diseases and insects are widely used for cultivation of *Olea europea* L. These are considered potential contaminants. Aim of this investigation lies in determination of concentrations of contaminants in several edible olive oils. All test samples were purchased in three consecutive seasons. They were analysed in compliance with standardized international protocols of wet digestion methods. Ion concentrations were determined in three replicates using method of inductively coupled plasma optical emission spectrometry. We have registered a positive correlation between storage time and heavy metals contents. It was particularly high in Iranian brands and varied significantly. Investigation results show that all obtained heavy metals contents in pepper-flavoured olive oil samples were significantly lower than in other samples. Considering the fungi-flavoured samples, levels of Pb and Cd were prominent and exceeded the maximum permissible level set in the majority of cases. The further monitoring is needed as all these metals are toxic and their detrimental effect becomes obvious only after several years of exposure.

Keywords: flavoured edible olive oil; inductively coupled plasma; toxic metals; food safety

Olive tree (*Olea europea* L.) is a subtropical commonly occurring in Mediterranean countries (Ziarati and Tosifi, 2014). In regards to the latest report issued by the European Commission (European Commission, 2012), olive oil is primarily manufactured in Spain (2.4 mil. ha), Italy (1.4 mil. ha), Greece (1 mil. ha) and Portugal (0.5 mil. ha). Vegetable oils are commonly utilized for cooking and food processing, as well as in cosmetics; furthermore, numerous products processed by pharmaceutical and chemical industries contain it (Covas, 2007; Pehlivan et al., 2008).

Cultural practices and control of diseases and insects represent essential aspects in provision of crop production efficiency (Shahgholi et al., 2015). They are potential sources of contamination. Contamination sources may also be related to wastes utilization (Vambol et al., 2018) or storage locations (Vambol et al., 2017). Application of nutrients is strictly important (CODEX STAN 33-1981, 1981). All products must comply with requirement of maximum contamination concentration limits established by the Codex Alimentarius Commission. Currently, following limits should be obligatory: the maximum concentration limit is 0.1 mg·kg-1 for lead (Pb); it is 0.1 mg·kg^{-1} for arsenic (As). United States Department of Agriculture (USDA) has also established the maximum permissible level of simultaneous heavy metals content equal to 0.1 mg·kg^{-1} for both Pb and As (Jafari Moghadam and Ziarati, 2016).

Several studies show that phenolic compounds have important role in preventing cardiovascular and neurodegenerative diseases, diabetes mellitus and cancer (Mailer, 2006; Waterman and Lockwood, 2007; Rodríguez-Morató et al., 2015). It is known that olive oil improves several cardiovascular risk factors, perhaps due to reduced level of plasma cholesterol and triglycerides (Huang and Sumpio, 2008; International Olive Council, 2012).

There are many different methods for analysing of various compounds of olive oils:

- liquid chromatography coupled with mass spectrometry for determination of sterols (Becerra-Herrera et al., 2014);
- liquid chromatography-triple-quadruple mass spectrometry for determination of phenolic compounds (Garcia Mesa and Mateos, 2007);
- pH-based flow-injection analysis system for determination of bitterness and total phenolic compounds (Godoy-Caballero et al., 2012);
- nonaqueous capillary electrophoresis with ultraviolet-visible and fluorescence detection for fast determination of phenolic compounds (Canabate-Diaz et al., 2007);
- high-performance liquid chromatography-mass spectrometry (HPLC-MS) for separation and determination of sterols and determination of heavy metals and trace elements by means of inductively coupled plasma atomic emission spectrometry (ICP-AES), inductively coupled plasma mass spectrometry (ICP-MS), atomic absorption spectrometry, inductively coupled plasma optical emission spectrometry (ICP-OES) (Covas, 2007; Flores et al., 2009; World Health Organization, 2011; Pehlivan et al., 2008; Zhang et al., 2014; Farzin and Moassesi, 2014).

Contact address: Parisa Ziarati, Nutrition and Food Sciences Research Center, Tehran Medical Sciences, Islamic Azad University, Tehran, Iran, 1941933111, e-mail: ziarati.p@iaups.ac.ir

Heavy metals may get into the human body with the food, fruits or vegetables. Currently, the highest concern of both the environmental and human health specialists is As contamination (Mirmohammad Makki and Ziarati, 2014). Predominant and also the most toxic form of this element under reductive conditions is As(III). Furthermore, concentration of dissolved arsenic in water rises with increasing water pH value (Singh et al., 2007). Pb is another toxic substance deteriorating multiple human body organs and systems. It has comparatively small range between safe exposure and fatal dose (United States Department of Agriculture, 2010). One more highly toxic element is cadmium (Cd) transferred to food from fertilizers and packaging (World Health Organization, 2011). The fourth heavy metal in the focus of this study is nickel (Ni), which is an essential trace metal for several animal species, microorganisms and plants (Council of Europe, 2001).

Primary goal of this paper is to determine contents of As, Pb, Cd and Ni in olive oil samples, both non-flavoured (virgin and extra-virgin) and flavoured (with fungi, aroma vegetables and pepper) ones, commercially available on Iranian market, and their comparison with Italian samples.

Toxic elements contents of olive oil samples are evaluated in terms of their potential to pose a health risk to consumers. Established elements concentrations were compared with the current legal standards applied in the European Union concerning heavy metals in food. Potential health effects are assessed in the light of the weekly intake limits of Pb, As, Cd and Ni set by the WHO and FAO of the UN (Codex Alimentarius Commission, 2001).

Material and methods

Olive oil samples for investigation were purchased in the selected areas of recognized markets in Iran and Italy. Samples were analysed using standardized international protocols of wet digestion methods. Every precaution necessary for preventing any sample contamination was taken (Singh et al., 2007; Jafari Moghadam and Ziarati, 2016). There were collected both non-flavoured (virgin and extra-virgin) and flavoured (with fungi, aroma vegetables and pepper flavours) olive oils. In total, 480 samples were randomly taken from food supply markets from the provinces of Lombardi in Italy and Tehran from Iran. All olive oil samples were purchased in autumn 2016 and later in winter and spring 2017. For each location, cultivars dominant in the respective area were selected. Olive samples were collected during the period appropriate for oil production. Single sample contained 500–1,000 g of fruits. These were manually collected from the same three trees and preserved at the temperature of +4 °C. Quantitative determination was made for heavy metals analysis. All containers used for sample collection were cleaned using liquid soap, rinsed with water, soaked in 10% nitric acid for at least one night, rinsed richly in deionized water and dried in order to avoid contamination. In order to ensure accuracy, certified standard reference material (Alpha – Line, Chem Tech Analytical, England) was applied. All recoveries of the metals observed exceeded 95%. Cd, Pb and Ni ion concentrations were determined in three replications by means of Varian Vista ICP-AES device. The intra-day (for samples collected during the same day) and inter-day (for samples collected during different days) precision and accuracy of the method were determined under the optimal working conditions by triplicate measurements of known Cd, Ni and Pb concentrations. The first standard stock solutions showed a 1.0 $mg \cdot l^{-1}$ concentration of each metal and aqueous standard solutions were prepared from them by means of appropriate dilution with 10% nitric acid. The working solutions showed concentration ranges of 0.001–0.1 ppm (Ziarati, 2012; Ziarati and Ghasemynezhad-Shanderman, 2014).

Quantitative determination of As

As(III) stock standard solution was prepared by weighing of 0.053 g of As_2O_3 which was dissolved in 1 mmol NaOH with concentrated HNO_3. Subsequently, its volume was made up to 100 ml with deionized water in the flask and the pH of solution was adjusted. At the same time, As(V) stock standard solution was made by weighing of 0.0551 g of As_2O_5 and its volume was adjusted to 100 ml with deionized water. The standard working solutions of 50 $\mu g \cdot l^{-1}$ of As(III) and As(V) were prepared by proper dilution of the stock standard solutions described above (Chooto et al., 2016).

Preparation of $NaBH_4$ solution

The solution of 0.4% $NaBH_4$ was used as reductant solution. It was prepared fresh each day by weighing of 1 g of $NaBH_4$ and 1.25 g of NaOH dissolved with deionized water up to a final volume of 250 ml (Chooto et al., 2016).

Preparation of samples

An aliquot of 3.0 g of each oil was weighed directly into the polypropylene containers. Subsequently, 1 ml of the 10% dilute nitric acid (Merck, 65%) and 0.5 ml of 30% H_2O_2 were added. The mixture of oil and acid was shaken at 50 Hz for 60 s with mixer in polypropylene containers until two layers were mixed thoroughly. All polypropylene containers were put in a shaking water bath at 60 °C for 1.5 hours. After centrifugation in special test tubes at 4,400 rpm for 8 min, the solution layer including lower acid was retreated with a pipette and filled by adding deionized water for up to a final volume of 25 ml. Then it was directly charged into the auto sampler of the ICP-AES device. After that, the determinations were performed at 228.802 nm wavelengths for Cd, at 220.353 nm for Pb, and at 231.604 nm for Ni.

Working conditions of ICP-AES device:

- Varian-Vista radio frequency power: 0.7–1.5 kW (1.2–1.3 kW for axial);
- plasma gas flow rate (Ar): 10.5–15 $l \cdot min^{-1}$ (radial) and 15 $l \cdot min^{-1}$ (axial);
- auxiliary gas flow rate (Ar): 1.5 $l \cdot min^{-1}$;
- viewing height: 5–12 mm;
- copy and reading time: 3 s (max. 100 s) and 1–5 s (max. 60 s), respectively.

For determination of inorganic As, emission signals of the As(III) can be registered at four wavelengths of 189.0 nm, 193.7 nm, 197.2 nm, and 288.8 nm. The highest intensity was revealed at 193.7 nm. The result was in good conformity with previous studies (Gettar et al., 2000).

Determination of inorganic and organic anionic arsenic compounds in water with ion chromatography method concerns hydride generation–inductively coupled plasma emission spectrometry, thus it was selected for the further experiments.

Total arsenic determination

Samples for investigation were prepared during total digestion in the following way. The first 0.5 g of dry weight sample was put into 50 ml centrifuge tubes of polypropylene. Next, 2.5 ml of Aristar nitric acid and 4 ml of Suprapur hydrogen peroxide were added to the sample. Then microwave digestion was done by means of CEM Mars5 Microwave System.

When digestion was conducted, dilution of sample was made with double distilled deionized water with rhodium (0.02 ml of solution with rhodium content of 10 $mg \cdot l^{-1}$) according to the internal standard. The volume of final diluted sample is 25 ml (Jafari Moghadam and Ziarati, 2016).

Analysis

An Agilent 7500c ICP-MS device was used to measure the content of As. Hydrogen was taken as collision and reaction gas. CEM Mars5 Microwave System was used to extract samples. For this purpose 1% Aristar nitric acid and 1% Suprapur hydrogen peroxide were taken (Ziarati and Tosifi, 2014). Extractable As was determined using the supernatant to improve chromatographic resolution. Such improvement was obtained because the supernatant oxidizes arsenite to arsenate which elutes at certain distance from monomethylarsonous acid (MMA) and dimethylarsinous acid (DMA), while arsenite elutes adjacent to MMA and DMA. Hamilton PRP X 100 anion exchange column using phosphate buffer was applied for analysis of As samples. T-piece was used to add solution of indium (0.01 $mg \cdot kg^{-1}$ content) in 1% nitric acid. The mentioned solution was taken as an internal standard (Jafari Moghadam and Ziarati, 2016).

Standard solution aliquots of 0.1 ml containing known amounts (10–100) $\mu g \cdot kg^{-1}$ of DMA were subjected to liquid chromatography coupled with ICP-MS method under the same conditions as the supernatants. Identification by retention time was performed by means of single sample standards of DMA, MMA and As(V). Calibration standard solutions including six As samples at different concentrations (1 ppb, 5 ppb, 10 ppb, 50 ppb, 100 ppb and 200 ppb) were made and analysed. The chromatogram for the 10 ppb calibration standard (5 µl injection) has shown that these six As samples were well enough separated in 4 min. The supernatant aliquots of 0.1 ml were applied into the column as they were. As quantification was carried out using peak areas.

Total As determination

Every 10th sample was selected for digestion. It was digested in duplicate and used for measurements. Each batch was collected from procedural blanks, spiked samples and certified reference materials (Jafari Moghadam and Ziarati, 2016).

Spiked samples were used for recovery estimate purposes. Spike recovery values ranged between 80% and 120% were taken as the mark to accept data. For a given sample the replicate values' relative standard deviation had to be less than 20%. Thus, each analytical batch had to provide reference material results within the certified range.

The limit of detection was established on the deviation equal to value of standard deviation of the signal from procedural blanks multiplied on three. Then its correction was made according to sample weight and dilution.

Statistical method

One-parametric Kruskal-Wallis/Mann-Whitney U tests were carried out in order to make comparison of differences between objects. Non-parametric multiple comparison test (Dunn's test) was utilized for specification of result statistical significance at $\alpha = 0.05$. The GLM procedure was carried out in order to analyse different metal treatments with means separated by Duncan's multiple range test at $p < 0.05$. Correlation analysis was performed using the CORR procedure with means separated at $p < 0.05$.

Results and discussion

Results were determined as dry weight of three replicates in each test in form of (mean value (MV) ± standard error (SE)). Samples were analysed with wet digestion method. Material preparation itself and analysis of heavy metals contents were all performed in accordance with standardized international protocols. Samples were analysed using ICP-AES method. Contents of Pb, Cd, Ni and As in samples of Italian olive oil are given in Table 1.

Obtained results revealed that the highest Pb concentration was registered in samples of Italian fungi-flavoured olive oil – 12.3301 ±0.112 $\mu g \cdot g^{-1}$. The lowest Pb concentration was registered in pepper flavoured sample being equal to 0.984 $\mu g \cdot g^{-1}$. The highest content of Cd was also registered in fungi-flavoured olive oil samples – 1.004 ±0.0123 $\mu g \cdot g^{-1}$. The highest detected

Table 1 Content of heavy metals in various samples of Italian olive oil, (MV ± SE) $\mu g \cdot g^{-1}$

Heavy metals	Olive oil samples flavoured with			Non-flavoured olive oil
	pepper	fungi	vegetable	
Pb	(0.984 ±0.091)	(12.3301 ±0.112)^{a}	(10.762 ±0.088)^{b}	(10.111 ±0.034)b
Cd	Not detectable	(1.004 ±0.0123)^{a}	(0.0876 ±0.004)^{b}	(0.0967 ±0.0054)b
Ni	Not detectable	(10.231 ±0.0143)^{b}	(12.349 ±0.128)^{b}	(14.180 ±0.011)a
As	(0.00020 ±0.00001)	(0.00040 ±0.00001)^{a}	(0.00030 ±0.00001)^{a}	(0.00040 ±0.00001)a

content of Ni was registered in non-flavoured olive oil – 14.180 ±0.011 μg·g^{-1} and the highest content of As was registered both in non-flavoured and fungi-flavoured oil samples. Four popular Iranian brands were selected and analysed. Data in Table 2 show that the highest content of Pb in Iranian olive oil was registered in the fourth brand – 18.783 ±0.016 μg·g^{-1}; the lowest content was registered in the third brand – 11.209 ±0.054 μg·g^{-1}. It can be clearly seen that the highest content of Cd was observed in the second brand – 4.181 ±0.042 μg·g^{-1}. Table 2 indicates that the fourth brand shows the highest Ni content – 14.444 ±0.2831 μg·g^{-1}. The highest amount of As was observed in the fourth brand – 0.0050 ±-0.0002 μg·g^{-1}.

Results of comparison of heavy metals content in Iranian and Italian samples are represented in Table 3. They show that Pb, Cd and As contents in investigated samples of Italian olive oil are significantly different in comparison to Iranian ones. All determined heavy metals were registered in Iranian olive oil samples with higher contents than in Italian ones, indicating that the risk assessment of olive oils consumed in Iran should be considered seriously. The content of Pb in all flavoured and non-flavoured Iranian oil samples was 14.944 ±0.045 μg·g^{-1}. This was merely 8.546 ±0.043 μg·g^{-1} in Italian oil samples, which is much lower. The content of Cd in Iranian oil samples was 3.362 ±0.032 μg·g^{-1}, which is ten times higher than in investigated Italian oil samples (p <0.005).

According to results of variance analysis of obtained data, Pb, Cd, Ni and As concentrations in olive oil samples were strongly influenced by specific origin of the producer. Flavour type also significantly affected the heavy metals content in Italian olive oil samples. There was a positive correlation registered between the olive oil manufacturing and quality level of packaging equipment – Iranian oil samples by new producers with modern equipment have shown lower heavy metals contents in majority of cases (p <0.05). Furthermore, there was observed a positive correlation between the storage time and heavy metals content. This interrelation was especially sharp for Iranian olive oil samples (Table 4) – heavy metals contents (especially Pb and Cd) in oils stored for twelve months were much higher in comparison with the freshly collected samples.

In general, it can be seen that the contents of Pb, Cd, Ni and As in Italian samples did not exceed the limits set by Codex Alimentarius and USDA. The mean amount of Pb in both groups exceeded the amount set by Codex Alimentarius and USDA, except for the samples flavoured by pepper (Jafari Moghadam and Ziarati, 2016). The mean content of Ni in Iranian brands was higher than in Italian brands, yet no significant differences were observed. Considering the mean content of Cd and As, they showed significant differences (p <0.05). The mean levels of Pb, Cd and Ni in Italian samples were lower than standards. Simultaneously, the As content in Iranian olive oil samples was a little higher than in Italian ones, however, both were lower than the maximum permissible level and showed no significant difference. The mean amount of Pb in both groups of samples exceeded those values set by Codex Alimentarius and USDA except for the pepper-flavoured samples (Jafari Moghadam and Ziarati, 2016). The mean content of Ni in Iranian olive oil samples was higher than in Italian ones, but results showed no significant differences in values. At the same time, results showed significant differences (p <0.05) in the mean content of Cd and As.

Investigation results showed that there was no detectable concentration of Cd in pepper-flavoured olive oil samples. Furthermore, the mean level of Cd content arises

Table 2 Content of heavy metals in various samples of Iranian olive oils, (MV ± SE) μg·g^{-1}

Heavy metals	Olive oil samples			
	series 1	series 2	series 3	series 4
Pb	(15.893 ±0.098)^{a}	(13.892 ±0.067)^{b}	(11.209 ±0.054)^{b}	(18.783 ±0.016)^{a}
Cd	(3.234 ±0.044)^{b}	(4.181 ±0.042)^{a}	(2.001 ±0.0022)^{c}	(4.032 ±0.014)^{a}
Ni	(12.354 ±0.036)^{b}	(10.542 ±0.072)^{c}	(9.786 ±0.0102)^{c}	(14.444 ±0.283)^{a}
As	(0.0040 ±0.0001)^{b}	(0.0030 ±0.0001)^{c}	(0.0030 ±0.0001)^{c}	(0.0050 ±0.0002)^{a}

Table 3 Content of heavy metals in Iranian and Italian olive oils, (MV ± SE) μg·g^{-1}

Olive oil samples	Heavy metals			
	Pb	Cd	Ni	As
Italian	(8.546 ±0.043)^{b}	(0.396 ±0.031)^{b}	(12.253 ±0.078)^{b}	(0.00020 ±0.00001)^{b}
Iranian	(14.944 ±0.045)^{a}	(3.362 ±0.032)^{a}	(9.579 ±0.065)^{a}	(0.0039 ±0.0002)^{a}

Table 4 Content of cadmium and lead during storage time in olive oil samples

Heavy metals	Storage time (months)			
	1	3	6	12
Pb	(14.221 ± 0.028)^{b}	(15.128 ±0.033)^{b}	(15.867 ±0.081)^{b}	(27.111 ±0.102)^{a}
Cd	(2.989 ±0.032)^{c}	(3.156 ±0.022)^{c}	(4.001 ±0.005)^{b}	(4.989 ±0.011)^{a}

to 1.004 ±0.0123 μg·g^{-1} in the fungi-flavoured olive oils, exceeding the maximum permissible level set by FAO and WHO. The mean contents of Cd in vegetable-flavoured and non-flavoured olive oils are equal to 0.0876 ±0.004 μg·g^{-1} and 0.0967 ±0.0054 μg·g^{-1}, respectively. Results showed no significant differences between them (p <0.05).

The Cd content was sharply registered in fungi-flavoured olive oil samples, which is probably related to contamination of fungi itself. It could also mean that peppers are stronger than fungi at removing the heavy metals and fungi may saturate metals more in terms of olive oils. Investigation results revealed that all heavy metals contents in pepper-flavoured olive oil samples were significantly lower than in other samples (p <0.03). The highest mean content of Ni was observed in non-flavoured samples. Results show no detectable content of Ni in pepper-flavoured olive oils. This significant difference is a very remarkable finding. The mean content of Pb in fungi-flavoured olive oil samples was 12.33 ±0.66 μg·g^{-1}; it was only 0.984 ±0.091 μg·g^{-1} in pepper-flavoured samples, which is 12.5 times less with significant difference (p <0.01). The ability of fungi to accumulate high concentrations of traces and some heavy metals is relatively unknown.

Conclusion

The results of investigation revealed that adding pepper to olive oil as a flavour significantly reduces heavy metals content. The further investigation of the heavy metals removal mechanism is strongly suggested. Nutrition and protection of vegetables and crops have to be performed properly. Heavy metals have toxic potential. However, their detrimental impact is shown in organism only after several years of being exposed to them. Observation of heavy metals in oil is vital, since it can help to develop preventive measures for avoiding excessive accumulation of them in human food chain. Companies treating products before selling them to markets should become aware of this and take the adequate steps for the manufacturing process improvement.

Acknowledgment

Authors acknowledge gratefully The Islamic Azad University, Tehran Medical Branch, Tehran, Iran.

References

BECERRA-HERRERA, M. – SÁNCHEZ-ASTUDILLO, M. – BELTRÁN, R. – SAYAGO, A. 2014. Determination of phenolic compounds in olive oil: New method based on liquid–liquid micro extraction and ultra-high performance liquid chromatography-triple–quadrupole mass spectrometry. In Journal of Food Science and Technology, vol. 57, no. 1, pp. 49–57.

CANABATE-DIAZ, B. – SEGURA CARRETERO, A. – FERNANDEZ-GUTIERREZ, A. – BELMONTE VEGA, A. – GARRIDO FRENICH, A. – MARTINEZ VIDAL, J. L. – DURAN MARTOS, J. 2007. Separation and determination of sterols in olive oil by HPLC-MS. In Food Chemistry, vol. 102, no. 3, pp. 593–598.

CHOOTO, P. – MUAKTHONG, D. – INNUPHAT, C. – WARARATTANANURAK, P. 2016. Determination of inorganic arsenic species by hydride generation–inductively coupled plasma optical emission spectrometry. In ScienceAsia, vol. 42, pp. 275–282.

CODEX ALIMENTARIUS COMMISSION. 2001. Report of the 33rd session of the codex committee on food additives and contaminants. Rome, Italy : Food and Agriculture Organization of the United Nations/World Health Organization, 289 pp.

CODEX STAN 33-1981. Standard for olive oils and olive pomace oils.

COUNCIL OF EUROPE. 2001. Guidelines on metals and alloys used as food contact material. France, Strasbourg : Council of Europe, 88 pp.

COVAS, M. I. 2007. Olive oil and the cardiovascular system. In Pharmacological Research, vol. 55, pp. 175–186.

EUROPEAN COMMISSION, Directorate-General for Agriculture and Rural Development Latest update: July 2012.

FA*RZ*IN, L. – MOASSESI, M. E. 2014. Determination of metal contents in edible vegetable oils produced in Iran using microwave-assisted acid digestion. In Journal of Applied Chemical Research, vol. 8, no. 3, pp. 35–43.

FLORES, J. C. M. – ORTIZ, M. D. – RUIZ, J. A. – PEINADO, F. M. – FERNANDEZ, I. G. 2009. Study of heavy metal and arsenic concentrations in olive farm soils, Sierra Mágina, Jaen, Spain. In Acta Agronomica, vol. 58, no. 4, pp. 303–307. (In Spanish: Estudio de metales pesados y arsénico en los suelos de olivar de Sierra Mágina, Jaén (España)).

GARCIA MESA, J. A. – MATEOS, R. 2007. Direct automatic determination of bitterness and total phenolic compounds in virgin olive oil using a pH-based flow-injection analysis system. In Journal of Agricultural and Food Chemistry, vol. 55, no. 10, pp. 3863–3868.

GETTAR, R. T. – GARAVAGLIA, R. N. – GAUTIER, E. A. – BATISTONI, D. A. 2000. Determination of inorganic and organic anionic arsenic species in water by ion chromatography coupled to hydride generation-inductively coupled plasma emission spectrometry. In Journal of Chromatography A, vol. 884, no. 1–2, pp. 211–221.

GODOY-CABALLERO, M. – GALEANO-DÍAZ, T. – ISABEL ACEDO-VALENZUELA, M. 2012. Simple and fast determination of phenolic compounds from different varieties of olive oil by nonaqueous capillary electrophoresis with UV-visible and fluorescence detection. In Journal of Separation Science, vol. 35, no. 24, pp. 3529–3539.

HUANG, C. L. – SUMPIO, B. E. 2008. Olive oil, the Mediterranean diet, and cardiovascular health. In Journal of the American College of Surgeons, vol. 207, no. 3, pp. 407–416.

INTERNATIONAL OLIVE COUNCIL. 2012. Health benefits of olives and olive oil. A review of the research commissioned by the International Olive Council, 11 pp.

JAFARI MOGHADAM, R. – ZIARATI, P. 2016. Reduction of arsenic content in imported polished rice: Association of cooking method. In Journal of Chemical and Pharmaceutical Research, vol. 8, no. 4, pp. 622–627.

MAILER, R. 2006. Chemistry and quality of olive oil. In Primefacts, vol. 227, pp. 1–4.

MIRMOHAMMAD MAKKI, F. – ZIARATI, P. 2014. Determination of histamine and heavy metal concentrations in tomato pastes and fresh tomato (Solanum lycopersicum) in Iran. In Biosciences Biotechnology Research Asia, vol. 11, no. 2, pp. 537–544.

PEHLIVAN, E. – ARSLAN, G. – GODE, F. – ALTUN, T. – ÖZCAN, M. 2008. Determination of some inorganic metals in edible vegetable oils by inductively coupled plasma atomic emission spectroscopy (ICP-AES). In Grasas y Aceites, vol. 59, no. 3, pp. 239–244.

RODRÍGUEZ-MORATÓ, J. – XICOTA, L. – FITÓ, M. – FARRÉ, M. – DIERSSEN, M. – DE LA TORRE, R. 2015. Potential role of olive oil phenolic compounds in the prevention of neurodegenerative diseases. In Molecules, vol. 20, pp. 4655–4680.

SHAHGHOLI, H. – MAKARIAN, H. – SHOKATI, B. – TALAEI, G. H. – ASGHARIPOUR, M. R. 2015. Do tillage methods affect germination and species similarity of soil weed seeds bank? In Acta Technologica Agriculturae, vol. 4, pp. 97–101.

SINGH, N. – KUMAR, D. – SAHU, A. P. 2007. Arsenic in the environment: Effects on human health and possible prevention. In Journal of Environmental Biology, vol. 28, no. 2, pp. 359–365.

UNITED STATES DEPARTMENT OF AGRICULTURE. 2010. United States standards for grades of olive oil and olive-pomace oil. United States, Washington : USDA, 19 pp.

VAMBOL, S. – VAMBOL, V. – BOGDANOV, I. – SUCHIKOVA, Y. – RASHKEVICH, N. 2017. Research of the influence of decomposition of wastes of polymers with nano inclusions on the atmosphere. In Eastern-European Journal of Enterprise Technologies, vol. 6, no. 10(90), pp. 57–64.

VAMBOL, S. – VAMBOL, V. – KONDRATENKO, O. – KOLOSKOV, V. – SUCHIKOVA, Y. 2018. Substantiation of expedience of application of high-temperature utilization of used tires for liquefied methane production. In Archives of Materials Science and Engineering, vol. 87, no. 2, pp. 77–84.

WATERMAN, E. – LOCKWOOD, B. 2007. Active components and clinical applications of olive oil. In Alternative Medicine Review, vol. 12, no. 4, pp. 331–342.

WORLD HEALTH ORGANIZATION. 2011. Arsenic in drinking-water: Background document for development of WHO guidelines for drinking-water quality. Switzerland, Geneva : World Health Organization, 24 pp.

ZHANG, P. – XIE, H. L. – ZHU, Q. H. – NIE, X. D. 2014. Determination of heavy metal elements in edible olive oil by ICP-MS. In Modern Food Science and Technology, vol. 30, no. 3, pp. 206–209.

ZIARATI, P. – GHASEMYNEZHAD-SHANDERMAN, S. S. 2014. Mineral contents in Pleurotus (Oyster Mushroom): Association of cooking method. In International Journal of Plant, Animal and Environmental Sciences, vol. 4, no. 2, pp. 496–501.

ZIARATI, P. – TOSIFI, S. 2014. Comparing some physical and chemical properties of green olive (*Olea europea* L.) in Iran association with ecological conditions. In International Journal of Plant, Animal and Environmental Sciences, vol. 4, no. 2, pp. 519–528.

ZIARATI, P. 2012. Determination of contaminants in some Iranian popular herbal medicines. In Journal of Environmental and Analytical Toxicology, vol. 2, no. 1, pp. 1–3.